1   **The largest arthropod in Earth history: insights from newly discovered *Arthropleura***

2   **remains (Serpukhovian Stainmore Formation, Northumberland, England)**

3   Neil S. Davies[1]*, Russell J. Garwood[2,3], William J. McMahon[1], Joerg W. Schneider[4,5], and

4   Anthony P. Shillito[1,6]

5   *[1]Department of Earth Sciences, University of Cambridge, Downing Street, Cambridge CB2*

6   *3EQ, United Kingdom.*

7   *[2]Department of Earth and Environmental Sciences, University of Manchester, Manchester*

8   *M13 9PL, United Kingdom.*

9   *[3]Earth Sciences Department, Natural History Museum, London SW7 5BD, United Kingdom.*

10   *[4]Technical University Bergakademie Freiberg, Institute of Geology, Department of*

11   *Palaeontology/Stratigraphy, Bernhard-von-Cotta-Straße 2, D-09596 Freiberg, Germany.*

12   *[5]Kazan Federal University, Institute of Geology and Petroleum Technologies, Kremlyovskaya*

13   *Street 18, Kazan, Russia.*

14   *[6]Current Address: Department of Earth Sciences, University of Oxford, South Parks Road,*

15   *Oxford, United Kingdom.*

16   * Corresponding author: nsd27@cam.ac.uk

17   **ABSTRACT**

18   *Arthropleura* is a genus of giant myriapods that ranged from the early Carboniferous to Early

19   Permian, with some individuals attaining lengths of over 2 metres. While most known fossils

20   of the genus are disarticulated and occur primarily in late Carboniferous (Pennsylvanian) strata,

21   here we report partially articulated *Arthropleura* remains from the early Carboniferous

22   Stainmore Formation (Serpukhovian; Pendleian) in the Northumberland Basin of northern

England. This 76 x 36 cm specimen represents part of an exuvium and is notable because only two comparably articulated giant *Arthropleura* fossils are previously known. It represents one of the biggest known arthropod fossils and the largest arthropleurid recovered to date, the earliest (Mississippian) body fossil evidence for gigantism in *Arthropleura*, and the first instance of a giant arthropleurid body fossil within the same regional sedimentary succession as the large arthropod trackway, *Diplichnites cuithensis*. The remains represent 12-14 anterior *Arthropleura* tergites, in the form of a partially sand-filled dorsal exoskeleton. The original organism is estimated to have been 55 cm in width and up to 2.63 m in length, weighing c. 50 kg. The specimen is preserved partially in three dimensions within fine sandstone and has been moderately deformed by synsedimentary tectonics. Despite imperfect preservation, the specimen corroborates the hypothesis that *Arthropleura* had a tough, sclerotized exoskeleton. Sedimentological evidence for a lower delta plain depositional environment supports the contention that *Arthropleura* preferentially occupied open woody habitats rather than swampy environments, and that it shared such habitats with tetrapods. When viewed in the context of all other global evidence for *Arthropleura,* the specimen contributes to a dataset that shows the genus had an equatorially restricted palaeogeographic range, achieved gigantism prior to late Palaeozoic peaks in atmospheric oxygen, and was relatively unaffected by climatic events in the late Carboniferous, prior to its extinction in the early Permian.

INTRODUCTION

The ancient giant myriapod *Arthropleura* is an instantly recognizable constituent of artistic reconstructions and museum dioramas illustrating the 'coal age' Carboniferous Period (359-299 Ma ago). Yet, despite the relative fame of these extinct animals, only two partially complete fossils of giant *Arthropleura* are presently known, both from Pennsylvanian (323-299 Ma) strata of Germany (Guthörl, 1934, 1935; Hahn et al., 1986; Schneider and Barthel, 1997; Schneider et al., 2010). Our understanding of *Arthropleura* otherwise draws on evidence

48   from rare presumed juveniles (Calman, 1915; Briggs and Almond, 1994; Almond, 1985),

49   disarticulated cuticular fragments (e.g., Andrée, 1913; Pruvost, 1930; Waterlot, 1934; Rolfe

50   and Ingham, 1967; Rößler and Schneider, 1997; Schneider and Werneburg, 1998; Wilson,

51   1999; Pacyna et al., 2012; Pillola and Zoboli, 2021), and wide *Diplichnites cuithensis*

52   trackways in contemporaneous strata (e.g., Briggs et al., 1979, 1984; Ryan, 1986; Pearson,

53   1992; Lucas et al., 2005; Schneider et al., 2010; Moreau et al., 2019).

54   The specimen described in this study is a 76 x 36 cm three-dimensional fossil and represents

55   the largest partially articulated *Arthropleura* fossil known thus far. It is from Late Mississippian

56   strata in northern England (Figures 1 and 2), making the specimen the earliest body fossil

57   evidence for arthropleurid gigantism. The unusual taphonomy, and potential significance and

58   implications of the fossil, necessitate an understanding of its stratigraphic,

59   palaeoenvironmental and tectonic context. In this paper we summarize these aspects, offer a

60   detailed description of the fossil's morphology, discuss its synapomorphies and thus taxonomic

61   placement, and finally place it into a global context of other known giant arthropleurids and

62   the Carboniferous world.

63   **GEOLOGICAL CONTEXT**

64   The fossil was discovered in January 2018 in a large (c. 2 x 3 x 8 metre) fallen block of

65   sandstone in coastal cliff outcrops at Howick Bay, approximately 10 km northeast of Alnwick,

66   Northumberland (55° 27' 19.2"N, 01° 35' 32.4"W) (Figure 3). Based on repeat visits to the

67   locality, it is likely that the block fell from the cliff between April 2017 and January 2018 and

68   has been gradually eroding since (most recent visit made in September 2021). The bed from

69   which the block fell is approximately 6 metres above beach level (Figure 4). The locality occurs

70   within a Site of Special Scientific Interest, and the fossil was extracted in May 2018 with

71   permission from Natural England and the landowners, the Howick Estate. It has been

72   accessioned by the Sedgwick Museum of Earth Sciences (specimen number CAMSM

73   X.50355).

74   *Basin setting*

75   The fossil bed occurs within the Stainmore Formation, deposited in the Northumberland Basin

76   during the mid-Carboniferous (Figure 3). At this time, northern Britain was in the foreland

77   region of the Variscan orogenic belt and had a basement topography characterized by a suite

78   of small subsiding sub-basins separated by structural highs.   The Northumberland Basin

79   comprises basinal lows of the Tweed Sub-Basin to the north and Northumberland Trough to

80   the south, separated in the middle by the structural high of the fault-bounded and granite-cored

81   Cheviot Block (Leeder et al., 1989; Chadwick et al., 1995; Fraser and Gawthorpe, 2003)

82   (Figure 3). As the Howick locality sits on the Cheviot Block, the Stainmore Formation reaches

83   only 228 metres thickness locally (Elliott, 1976), compared to 500 metres in basinal lows (Dean

84   et al., 2011).

85   *Age*

86   The Stainmore Formation is the youngest constituent unit of the Visean Yoredale Group,

87   overlying the Alston Formation and, below this, the Tyne Limestone Formation (Dean et al.,

88   2011) (Figure 3C). The formations of the Yoredale Group comprise repeating cyclothems of

89   sandstones, shales, coals and limestones, but are differentiated by an upwards-decreasing

90   frequency of carbonates as the units become increasingly dominated by terrigenous strata

91   (Reynolds, 1992; Frank and Tyson, 1995; Dean et al., 2011; Booth et al., 2020).

92   Transgressive limestone marker horizons (with local lithostratigraphic names) occur

93   throughout the Yoredale Group (Tucker et al., 2009; Waters et al., 2014; Booth et al., 2020)

94   and can be biostratigraphically correlated to regional substage level throughout northern

95   England and Scotland, using miospore and foraminifera assemblages (Turner and Spinner,

96   1992; Cózar and Somerville, 2012, 2020, 2021; Ingrams et al., 2020). The fossil-bearing bed

97   occurs two metres stratigraphically below the Lickar Limestone (formerly 'Howick

98   Limestone'; Farmer et al., 1970; Elliott, 1976), and above the Cushat Limestone. Although

99   these marker beds are dolomitized and lack biostratigraphically useful taxa, they both occur

100 above the Great Limestone (early Pendleian) and below the Sugar Sands Limestone (earliest

101 Arnsbergian) (Cózar and Somerville, 2020), and the Lickar Limestone is thus considered to

102 mark the base of the late Serpukhovian (Cózar and Somerville, 2021). Accordingly, the fossil-

103 bearing bed can be confidently determined to have been deposited during the Pendleian

104 regional substage, dating it to approximately 326 Ma, within the latest early Serpukhovian

105 (Heckel and Clayton, 2006; Richards, 2013; Cohen et al., 2021).

106   *Local structure*

107 The fossil and its host bed are strongly influenced by the adjacent Howick Fault; a major east-

108 west directed normal fault extending inland from the coast for 10 km, with a vertical

109 stratigraphic displacement of 200 metres downthrown to the south (Westoll et al, 1955; Farmer

110 and Jones, 1969; Kjemperud, 2011; Burt and Tucker, 2020). At Howick Bay the fault directly

111 juxtaposes the Stainmore Formation against the Alston Formation, and 20 metres of the total

112 vertical displacement has been accommodated within a 100 metre-wide damage zone, where

113 the hanging-wall and foot-wall are dissected by multiple small antithetic and synthetic faults.

114 The fossil bed itself is sandwiched between several such faults in the hanging-wall (Figure 3E).

115   *Sedimentological and palaeoenvironmental context*

116 Most of the strata exposed at Howick Bay belong to the Visean Alston Formation (Figure 3)

117 and are typified by marine limestones and storm- and tide-deposited siliciclastic strata

118 (Reynolds, 1992; Booth et al., 2020; Allport et al., 2021). At the southern end of the bay, the

119 Howick Fault juxtaposes these against the younger strata of the Stainmore Formation, in which

120   the fossil was discovered, and which yield a greater abundance of signatures of non-marine

121   deposition, amongst less frequent limestones and tidally influenced siliciclastic strata.

122   The section has been well studied from a sedimentological perspective (Farmer and Jones,

123   1969; Elliott, 1976; Scarboro and Tucker, 1995), and the Stainmore Formation can confidently

124   be interpreted as being deposited in a littoral deltaic setting (note that although it has recently

125   been purported to contain a fairweather- to storm-wave base ichnofauna (Boyd and McIlroy,

126   2016, 2017, 2018), locality details in these papers show that the described trace fossils occur

127   north of the Howick Fault, within the Alston Formation).

128   The Stainmore strata that immediately underlie the fossil horizon contain signatures of tidally

129   influenced sedimentation, including possible tidal rhythmites burrowed with *Skolithos,*

130   *Teichichnus* and *Taenidium* (Figures 5 and 6), siderite nodules, and a prominent heterolithic

131   lateral accretion set that likely records a small tidal channel (Scarboro and Tucker, 1995;

132   Davies and Gibling, 2013). These strata are interbedded with sandstones and thin coals

133   deposited in a lower delta plain setting, revealed by signatures including plant root traces, wave

134   ripple marks, mudcracks and a bedding plane that exposes a *Baropezia* trackway (Scarboro and

135   Tucker, 1995; since degraded by wave erosion; Fig. 6A-B), attributable to an anthracosaur

136   tetrapod (Falcon-Lang et al., 2006).

137   The fossil bed itself is a gently channelized coarsening-up package of amalgamated sandstones,

138   3.2 metres in thickness, and most easily studied in the recently fallen block. The lower half of

139   the package comprises horizontally bedded fine-grained sandstone laminae that are disrupted

140   by plant root traces, including *Stigmaria*. These are succeeded by sandstone laminae that are

141   notably wave ripple-marked and colonized with horizontal burrows (*Planolites*) and

142   meandering grazing trace fossils (*Archaeonassa*), before the appearance of the 1 metre-thick

143   package of trough cross-bedded medium-grained sandstone, within which the fossil was fully

144   interred.

145   In addition to the giant arthropod fossil, the cross-bedded package also hosts abundant plant

146   debris from multiple different taxa (Figure 6), including: 1. A thin axis that bifurcates at an

147   acute angle distally (possibly being the proximal part of a pteridosperm frond) (Fig. 6F); 2.

148   *Lepidodendron (sensu lato)* bark fragments (Fig. 6F); and 3. Large seeds, possibly *Samaropsis*,

149   which were produced by cordaitaleans (Fig. 6G). Both the top and base of the cross-bedded

150   package are mantled with *Stigmaria* roots (Fig. 6H). The bed has previously been interpreted

151   (without access to the fallen block) as recording a crevasse channel deposit (Elliott, 1976) or a

152   small delta infilling a shallow embayment on the lower delta plain (Scarboro and Tucker,

153   1995). However, here we favour the interpretation of deposition by a minor fluvial channel,

154   based on the abundance of non-marine biological detritus within the cross-bedded sands and

155   the fact that it is stratigraphically sandwiched between surfaces that were stabilized by lycopsid

156   tree roots.

157   The strata that immediately overlie the fossil bed are less readily studied in the field: at the

158   precise fossil locality they either occur in the inaccessible upper part of the cliff face, or are

159   faulted out, and in the southernmost part of Howick Bay they are eroded out at an incised

160   channel bounding surface. Midway between these points, the overlying strata crop out at beach

161   level as nondescript carbonaceous shales with siderite nodules, which yield bryozoans,

162   brachiopods, crinoids and marine foraminifera (Scarboro and Tucker, 1995; Cozar and

163   Somerville, 2020). Above this transgressive package, the stratigraphic top of the Howick Bay

164   section is characterized by 8 metres of fully non-marine braided fluvial sandstones, which can

165   be traced for 3 km south of Howick Bay, and which have incised a channelized base at least 4

166   metres into the underlying strata (Farmer and Jones, 1969; Elliott, 1976). The sedimentological

167 context of the fossil-bearing bed is thus diagnostic of a non-marine fluvial channel, in

168 immediate proximity to the marine shoreline.

169 **SYSTEMATIC PALAEONTOLOGY**

170 Phylum ARTHROPODA von Siebold, 1848

171 Subphylum MYRIAPODA Latreille, 1802

172 Order ARTHROPLEURIDA Waterlot, 1934

173 Family ARTHROPLEURIDAE von Zittel, 1885

174 Genus *Arthropleura* Jordan in Jordan & Meyer, 1854

175 Type species: *Arthropleura armata* Jordan, 1854, p.13-15, pl. 2, figs. 4-5 in Jordan and v.

176 Meyer, 1854, *Arthropleura* sp. Jordan in Jordan & Meyer, 1854

177 (Figs. 1 and 2)

178 Material - CAMSM X.50355, partial remains comprising articulated anterior 12-14 tergites in

179 two slabs.

180 Locality - Howick Bay (55° 27' 19.2"N, 01° 35' 32.4"W), Northumberland, England.

181 Age and formation - Early Serpukhovian, Stainmore Formation (Yoredale Group).

182 Description – specimen identified as the partial anterior dorsal exoskeleton of *Arthropleura*

183 because of trilobate tergites, coupled with large dimensions. Remains comprise 12-14 tergites

184 and paratergites, 76 cm in maximum length from the anterior to posterior, and 36 cm at greatest

185 width. Preserved as three-dimensional cuticular infill by sand, with limited cuticular material.

186 Ornamentation limited: some longitudinal striae visible on paratergites and a granular or

187 verrucose texture on anterior margins of medial tergites. Specimen has irregular morphology

188 owing to the taphonomy of a large three-dimensional exoskeleton interred within sand in a

189 tectonically active setting.

190 **DESCRIPTION OF THE SPECIMEN**

191 The three-dimensional preservation of this large fossil is summarised in Figure 7. The fossil is

192 visible on a fracture surface within a block of cross-bedded fine-grained sandstone. The

193 fracture splitting the well-indurated host lithology is recent and presumably formed when the

194 host block fell from the cliff. The fossil is preserved on surfaces either side of this fracture.

195 As the fracture may run through the middle of the three-dimensional fossil (see later discussion)

196 it is inappropriate to refer to these as part and counterpart (Figure 1), and they are here referred

197 to as Slab A and Slab B. Slab A is the upper stratum and hosts the bulk of the fossil. Slab B is

198 the lower stratum and preserves an impression that domes upward to a relief of c. 10 cm,

199 creating a three-dimensional semi-cylindrical form.

200 The fossil comprises 12-14 sub-rectangular medial tergites, flanked on one side by right

201 paratergites. The left paratergites are missing, and the medial tergites terminate against a

202 serrated edge. The right paratergites have frayed and irregular lateral margins, and so are also

203 imperfectly preserved (Figures 2 and 8). The anterior 5-6 paratergites are increasingly recurved

204 (Figures 1 and 2).

205 Slab A broke into several pieces during extraction from the host block; these fragments reveal

206 the three-dimensional form of the tergites. Each is filled with the host sediment, forming three-

207 dimensional imbricated pillows. The tergite sand-infills are 4 mm thick in the medial tergites,

208 thinning to 1 mm or less towards the paratergites (Figure 9).

209 The fossil is overlain in Slab A, and underlain in Slab B, by a carbonaceous smear that exactly

210 mirrors the form of the frayed right paratergites (Figure 10). The offset between recognisable

211 frayed paratergites, and their displaced form in smears can be measured. Offset is consistent

212 along the length of the fossil at 40 cm. Excluding the smear repetition, the total length of the

213 fossil is 76 cm and its maximum preserved width from right lateral paratergite to termination

214 of left medial tergite is 36 cm.

215 In addition to this smear, remnants of carbonaceous material can be seen in patches on both

216 slabs, most notably in the tergal margins in Slab A (Figure 9), where the arthrodial membrane

217 would have been present in life. The stratigraphically upper (and dorsal) side of the tergites in

218 Slab A can be seen, in broken fragments, to be carbon-rich and flecked with abundant micas,

219 which possibly adhered to a sticky surface prior to burial (Figure 8). The majority of the fossil,

220 however, has no organic material and its form is revealed by impression, or sand-infill, alone.

221 Due to the lack of well-preserved cuticle and granular nature of the host sediment,

222 ornamentation is not consistently visible on the specimen. However, the anterior margins of

223 the medial tergites - where the segments would have been joined by softer arthrodial membrane

224 - have a rough, grainy appearance on the surfaces of both slabs. The absence of this texture

225 across the remainder of the fossil and host sediment implies either it is an original texture, or

226 that it is a taphonomic difference reflecting the contrasting nature of the exoskeleton between

227 these regions (Figure 8). Additionally, striae can be seen on some of the paratergites, some of

228 which appear to form pronounced medial grooves that are parallel with the central axis of a

229 paratergite (Figure 8).

230 The above information can be combined to describe a stratigraphic transect upwards through

231 the fossil as follows: 1. 10 cm of domed fine-grained sand (Slab B); 2. Negligible thickness,

232 offset carbonaceous smear (Slab B); 3. Impression fossil of tergites/paratergites, with grainy

233 and striated surface textures (Slab B); 4. Remnant patches of organic material and original form

234 of tergites, recording verrucose and striated surface textures (Slab A); 5. 1-4 mm thickness of

235 sand infill within three-dimensional tergites (Slab A); 6. A highly micaceous and carbonaceous

236   veneer on the upper side of the tergites (Slab A); 7. Negligible thickness, offset carbonaceous

237   smear (Slab A); 8. Overlying fine-grained sand (Slab A).

238   **TAPHONOMY OF THE SPECIMEN**

239   The granular sandy host lithology of the specimen is remarkably coarse for preserved

240   arthropleurid remains. All other articulated remains are known from very fine-grained

241   mudrocks, sandy siltstones or crystal tuffs (Guthörl. 1934, 1935; Hahn et al., 1986; Schneider

242   and Barthel, 1997; Schneider et al., 2010), although several isolated remains from the late

243   Visean Hainichen basin in Saxony are well preserved in silty fine-grained sandstones to fine-

244   to medium-grained sandstones (Rößler and Schneider, 1997). The well-sorted, granular nature

245   of the host sediment created taphonomic conditions that were not conducive to preserving

246   chitinous cuticles in high fidelity (Briggs et al., 1998) and the fossil is identifiable primarily

247   because the cuticle was filled with sediment post mortem. The only evidence for original

248   organic material is some carbonized material between the tergites in Slab A (Figure 9A), and

249   the carbonaceous and micaceous material that appears offset and smeared across both the

250   ventral and dorsal extremes of the fossil.

251   *Missing body parts*

252   The Howick specimen preserves only part of the dorsal exoskeleton of the organism, with no

253   evidence of appendages. As is common to all other reports of giant *Arthropleura*, the head is

254   also missing, but the lack of segmentation anterior to the first sizable tergite suggests that the

255   fossil may terminate where the head capsule was during life (Figure 2). No trace of appendage

256   attachment points is present on either side of the specimen preserved in Slab A, where both the

257   ventral and dorsal surfaces of the dorsal exoskeleton can be observed. The most plausible

258   explanation for these characteristics is that the specimen is an exuvium, potentially one in

259   which the suture was located between the ventral edge of the paratergite and the body. This

260 scenario would have resulted in a hollow mass of cuticle representing the dorsal and lateral

261 exoskeleton, which was open to sediment infilling during an interval after moulting but prior

262 to ultimate internment in the sediment pile.

263 Despite missing key body parts, the remains are not fully disarticulated, which is unexpected

264 given the sedimentological evidence for relatively high energy deposition, as arthropod

265 exoskeletons rapidly disarticulate when tumbled in a fluid (McCoy and Brandt, 2009).

266 Considered alongside the fact that the fossil is preserved in three dimensions, fully enveloped

267 and partially coiled (longitudinal doming of the underlying sediment in Part B) within a fine-

268 grained cross-bedded sandstone, this suggests that the remains were instantaneously deposited

269 with the host sediment. In a scenario where the fossil was parautochthonous, with the exuvium

270 discarded and filled with sand away from the final resting location, this could feasibly have

271 occurred as a pulse of bank margin debris (i.e., sand, exuvium, and plant remains) that collapsed

272 into a river channel and was subsequently sculpted by migrating bedforms.

273 Two further characteristics imply that the fossil represents an articulated exuvium that had

274 already degraded prior to such collapse and interment: 1. The absence of any other fragments

275 of arthropleurid material within the host bed (despite intensive searching), which implies that

276 a complete organism was not disarticulated within the bedform in which it was ultimately

277 preserved; and 2. The degradation recorded by the serrated left lateral margin to the tergites,

278 and the irregular broken appearance of the majority of the right paratergites (Figures 1 and 2).

279   *Post burial deformation*

280 Two key characteristics of the fossil imply that it has been deformed post burial. First, the sand

281 filled tergites in Slab A can be seen to buckle, suggesting that they experienced compressional

282 stress within the sediment pile. Second, the repetition of form between the carbonaceous smears

283 that sandwich the fossil and the sand infill implies that the internal cast has been squeezed out

284   and offset from the dorsal and ventral cuticle after partial lithification. Both characteristics are

285   unusual but can be readily explained through the tectonic taphonomy of the host bed.

286   The fossil-bearing bed occurs within the hanging-wall damage zone of the Howick Fault

287   (Figure 4), and has previously been imaged, when still *in situ* in the cliff face, in earlier

288   structural geology investigations of the locality (see De Paola et al., 2005, their Fig. 8;

289   Kjemperud, 2011, their Figs. 14 and 17). The Stainmore Formation in the hanging-wall damage

290   zone contains several features, including small thrust faults, listric geometries, hanging wall

291   stratal thickening, mudstone deformation, and calcite veins, that together show that the master

292   fault was syn-depositional and occurred when the sediment was only partially lithified (De

293   Paola et al., 2005; Kjemperud, 2011). Normal faulting in the Howick Fault Zone was initiated

294   during thermal subsidence after the earliest Carboniferous cessation of rifting in the

295   Northumberland Basin and was contemporaneous with the deposition of the Yoredale Group

296   (Kimbell et al., 1989; De Paola et al., 2005; Kjemperud, 2011). Development continued when

297   it was reactivated as a strike-slip fault during Variscan-induced shortening (Leeder et al., 1989;

298   Chadwick et al., 1995; Fraser and Gawthorpe, 2003; De Paola et al., 2005), as well as during

299   the Carboniferous-Permian emplacement of the adjacent Whin Sill dolerite (De Paola et al.,

300   2005; Kjemperud, 2011).

301   Fault development at the precise fossil locality thus involved near-continual deformation of the

302   host sediment, prior to full lithification, throughout the Carboniferous and into the Permian. To

303   accommodate the stress in the synsedimentary main fault, internal compressional strain in the

304   fossil-hosting bed would have occurred, and the arthropleurid fossil – as a significantly large

305   material discontinuity within the un/partly-lithified sandstone bed – likely took up some of this

306   strain, buckling the tergites and offsetting the internal sand moulds from the carbonized

307   remains of the exuvium.

INTERPRETATION OF ARTHROPLEURID IDENTITY

308

309 The partial preservation of cuticular material, segmented nature of this fossil and partial

310 preservation of lateral divisions of the segments into medial- and paratergites strongly supports

311 an arthropod identity for this fossil, even though no appendages are preserved. The morphology

312 of the best preserved paratergites (i.e., 4-6; Figure 2) indicates that the fossil records the anterior

313 part of the animal.

314 The surface of Slab A is interpreted as recording the ventral surface of the dorsal exoskeleton,

315 with the surface of Slab B recording a three-dimensional counter-print of this, and the pillow-

316 forms in Slab A being sand infills of the tergites. The dorsal surface of the dorsal exoskeleton

317 is visible in some fragments that have broken off from Slab A (Figure 8C).

318 No other Carboniferous arthropods with this morphology, or of this size, are known: thus, based

319 on these observations, we propose that this fossil represents a giant arthropleurid. Whilst it is

320 possible that other – yet unreported - arthropod taxa reached this size during the Carboniferous,

321 an identity as *Arthropleura* sp. remains the most parsimonious explanation. Additionally, two

322 characteristics of the specimen bear notable resemblance with other specimens of

323 *Arthropleura*: 1) the recurvature of the anterior paratergites is similar to that seen in other

324 specimens (Hahn et al., 1986; Briggs and Almond 1994; Brauckmann et al., 1997; Kraus and

325 Brauckmann, 2003; Schneider and Werneburg, 2010) ; and 2) the granular surface texture on

326 the anterior border of the tergites bears resemblance to that visible in partial specimens

327 (Brauckmann et al., 1997).

328 Five morphospecies of *Arthropleura* have previously been described, mainly based on cuticular

329 ornamentation: *A. armata* and *A. mammata* are in common use (e.g., see Hahn et al., 1986),

330 and there are less frequent or isolated reports of *A. cristata* (Hannibal, 1997), *A. fayoli* (Boule,

331 1893), and *A. maillieuxi* (Pruvost, 1930). Comparable large arthropleurids have been assigned

332   to the species *A. armata,* but the lack of preserved appendages or detailed ornamentation in the

333   Howick specimen precludes confident species-level diagnosis.

334   *Original size*

335   Assuming that the missing left paratergites were the same size as those preserved on the right,

336   the original carcass must have been at least 55 cm in width, and well more than the 76 cm

337   length that is preserved. A number of alternative width:length ratios for *Arthropleura* have

338   been posited, calculated on the basis of trackways and partial giant, or complete juvenile,

339   specimens with appendages. Estimates range between 3.47 (Martino and Greb, 2009), 3.75

340   (Ryan, 1986), 3.6-4.4 (Kraus, 1993; Schneider and Werneburg, 1998; Schneider et al., 2010)

341   and 4.78 (Hahn et al., 1986). The Howick specimen is the widest arthropleurid fossil thus far

342   discovered. Based on these ratios, it would also represent the largest individual discovered to

343   date – being between 190 and 263 cm in length (Figure 11). We contend that the true size is

344   most likely to have been at the upper end of these estimates because the fossil has been

345   tectonically compressed and only 12-14 tergites are preserved.

346   Estimates of the number of tergites in *Arthropleura* have improved with the discovery of new

347   specimens, but all estimates are considerably greater than the 12-14 in the specimen described

348   here. Early morphological details were based on the description of a ~6.5 cm long, nearly

349   complete, juvenile specimen (Calman 1915) from below the Top Hard Coal in Derbyshire,

350   England (late Bashkirian; Duckmantian (Sheppard, 2005)). That specimen has an indistinct

351   head region, a nearly complete trunk in dorsal aspect, and an indistinct terminal segment,

352   permitting the recognition that *Arthropleura* had at least 28 tergites (Calman, 1915). Several

353   subsequent reconstructions (e.g. Rolfe and Ingham, 1967, Fig. 2; Briggs et al., 1984) were

354   strongly influenced by the ~90 cm long 'Maybach specimen' from the Moscovian Saarbrücker

355   Schichten (Sulzbach Formation, Saarbrücken Subgroup) of the Saar Basin, Germany (Guthörl,

1935; first described and figured in detail by Hahn et al., 1986, Fig. 1 and pls. 1, 2). That specimen shows 23 tergites from a dorsal aspect, but the head and tail regions are missing (ibid., pl. 2). Hahn et al. (1986, Fig. 2) suggested these represent the remains from a trunk of an estimated 30 tergites. Other discoveries that inform on *Arthropleura* segment numbers include two associated remains of a distorted ventral exoskeleton from the Gzhelian-Asselian Döhlen Formation of Saxony, which preserve 25 articulated leg bearing segments of an individual between 0.65 m to 0.8 m in length (Schneider and Barthel, 1997, p. 195, pls. 5 - 7). The most recent reconstructions of *Arthropleura* - a 2.20 m long 3D-reconstruction, figured by Schneider and Werneburg (2010, fig. 6C) and that is presented here (Fig. 11A) - assume 32 tergites for adult giant arthropleurids. All of these reconstructions imply that the Howick specimen comprises less than half the length of the original organism.

The Howick specimen is thus analogous in size to the very largest *Arthropleura* previously interpreted from indirect evidence: the 51 cm wide organism interpreted from fragmentary preserved appendages in the Gzhelian-Asselian Manebach Formation, Germany (Schneider and Werneburg, 1998), and the organisms that left nearly 50 cm wide trackways in the Visean Strathclyde Group of Scotland (Pearson et al., 1992; Pearson and Gooday, 2019) and Gzhelian Cape John Formation of Nova Scotia (Ryan, 1986; Ryan and Boehner, 1994).

Weights of 8-10 kg have previously been calculated for giant *Arthropleura*, estimated from interpretations of a fraction of a simplified cylindrical volume and a density equivalent to that of water (Kraus and Brauckmann, 2003). However, a cylinder is not representative of the true form of *Arthropleura*, which is better envisaged as a hemi-ellipsoid with a flat underside and raised topside tapering towards the lateral, anterior and posterior edges. Additionally, the density of water (997 kgm^{-3}) is not representative of the densities of modern giant millipedes, which are typically 350-550 kgm^{-3} (Bercovitz and Warburg, 1985; Mwabvu et al., 2010; Horváthová et al., 2021).

381 We have calculated two possible estimates for the weight of the Howick *Arthropleura* based

382 on a reasonable estimate of 20 cm as the height, and consequent dimensions of 20 cm x 55 cm

383 x 263 cm. Calculating this volume as a hemi-ellipsoid (volume = 2/3 πabc, where a, b and c

384 are half height, width and length) equates to approximately 158,000 cm^3, suggesting substantial

385 weights of c. 55-87 kg, based on the densities of extant giant millipedes. This method provides

386 a replicable estimate but does not account for the true organism shape being a fraction of a

387 complete hemi-ellipsoid. To account for the likely overestimate, we also purchased a

388 commercially available 3D mesh of a model *Arthropleura* from Turbosquid.com, loaded this

389 into Blender (Garwood and Dunlop, 2014), and scaled it to the dimensions derived from this

390 fossil (see Supplementary Information). The 3D Print Toolbox in Blender provided a volume

391 measurement for an *Arthropleura*-shaped object with the specified dimensions, of 91,509 cm^3.

392 equivalent to c. 32-50 kg, based on the densities of extant giant millipedes. This range of

393 estimates converges at an approximate weight of around 50 kg, which is substantially larger

394 than previous estimates, but inevitable due to the extreme size of this specimen (applying Kraus

395 and Brauckmann's (2003) calculation method would lead to an implausible weight estimate of

396 c. 205 kg).

397 With a surface area of c. 2.7 m^2, the Howick specimen is one of the largest individual arthropod

398 fossils found to date globally, comparable with the largest specimen of the Ordovician trilobite,

399 *Isotelus rex* (Rudkin et al., 2003). It may also record the largest known arthropod in Earth

400 history. The upper size estimate of 2.63 m length and c. 50 kg in weight exceeds the 2.5 metre-

401 length interpreted for *Jaekelopterus rhenaniae*, the Early Devonian eurypterid previously

402 suggested to be the largest arthropod ever to have evolved (Braddy et al., 2008).

403 **IMPLICATIONS FOR THE UNDERSTANDING OF *ARTHROPLEURA***

404   The Howick specimen provides limited new information on *Arthropleura* Bauplan, being

405   primarily the ventral surface of the dorsal exoskeleton. The specimen lacks the ornamentation

406   of arthropleurid remains that are found in more taphonomically favourable settings (indeed,

407   these would not be expected on the ventral surface of the dorsal exoskeleton). Despite this

408   limited detail, the curvature of the specimen supports assertions of arthropleurid

409   manoeuvrability and refutes the suggestion that *Arthropleura* may have had a weak,

410   unmineralized cuticle, and was stabilized by musculature and antagonistic hydraulics as in

411   caterpillars (e.g., Kraus and Brauckmann, 2003; Kraus, 2005; McGhee, 2018). The fractured

412   margins and sand-infill of the tergites in the Howick specimen imply a sclerotized exoskeleton

413   in life, as does the survival of an exuvium. Further supporting evidence is provided by

414   arguments based on trackways, where leg stance (Shear and Edgecombe, 2010) and track depth

415   (Lucas et al., 2005; Schneider et al. 2010) suggest skeletal support was offered by more than

416   just haemolymph pressure, and the observation that arthropleurid remains are more recalcitrant

417   than other arthropod fragments in depositional settings with significant transport histories

418   (Proctor 1998).

419   *Arthropleurid habitat*

420   The fossil-bearing bed was deposited in a minor fluvial distributary channel in direct proximity

421   to the coast, and the completeness of the arthropleurid fossil suggests that it has not been subject

422   to a significant history of transport. Direct palaeobotanical evidence shows that the small river

423   traversed a lower delta plain that was colonized by a mixed arborescent flora of lycopsids,

424   medullosalean pteridosperms and cordaitaleans (Figure 6). The presence of only thin,

425   discontinuous and infrequent coals implies that the vegetation was relatively open at the coast,

426   rather than forming dense coal forests (at 326 Ma old, the fossil also pre-dates the widespread

427   dominance of equatorial wetland coal forests in Euramerica; Greb et al. 2006). Ichnological

428   evidence shows that the lower delta plain also hosted communities of terrestrially adapted

429   amphibians and small infaunal and surface-grazing invertebrates (Figure 6), while adjacent

430   marine waters were populated by a normal-salinity community of vertical burrowers,

431   bryozoans, brachiopods, crinoids and marine Foraminifera.

432   This setting contrasts with the traditional view that arthropleurids predominantly occupied

433   swampy environments (e.g., Donovan, 2002; Kraus and Brauckmann, 2003). Although even

434   early investigations noted that *Arthropleura* was more common in fluvial sandstones that were

435   intercalated with coals (Guthörl, 1940), the common perception of an association of

436   *Arthropleura* with coal swamp environments appears to have arisen as an artefact of the earliest

437   fossil discoveries of the organism being made in working coal mine settings and excavation

438   dumps (e.g., Guthörl, 1936). The interpretation of tightly vegetated coal-forming swamps as

439   the preferred habitat of *Arthropleura* is not supported by finds of more or less allochthonous

440   body remains and especially not by the absolutely autochthonous *Arthropleura* tracks

441   (Schneider et al., 2010). A wealth of more recent ichnological evidence is aligned to the setting

442   recorded by the Howick example, namely sparsely wooded, alluvial and littoral environments

443   (e.g., Pearson et al., 1992, 2020; Lucas et al., 2005; Schneider et al., 2010; Getty et al., 2017).

444   Additionally, the close proximity of the fossil to the trackway *Baropezia* (Scarboro and Tucker,

445   1995) provides direct evidence that confirms that arthropleurids shared an environmental niche

446   with tetrapods, even by the end Mississippian (Falcon-Lang et al., 2006; Martino and Greb,

447   2009; Schneider et al., 2010, Minter et al., 2016, Getty et al., 2017, Dernov, 2019), contrary to

448   the traditional view that the latter would have outcompeted them (e.g. DiMichele et al., 1992).

449   Ichnological evidence that has been attributed to arthropleurid activity includes the large

450   trackways *Diplichnites cuithensis* (e.g., Briggs et al., 1979, 1984; Ryan, 1986; Pearson, 1992;

451   Schneider et al. 2010, Moreau et al., 2019), possible large *Beaconites* aestivation burrows

452   (Falcon-Lang et al., 2006; Falcon-Lang and Miller, 2007; Pearson and Gooday, 2019) and rare

453   coprolites (Scott and Taylor, 1983). The identification of an arthropleurid tracemaker for many

454   of these ichnofossils is assumed primarily based on their size, and sites that yield both trace

455   and body fossils are thus far unknown (Table 1). Trace fossil localities have a different bias to

456   body fossil localities, requiring the presence of true substrates (bedding planes that have

457   archived ancient air-substrate interfaces) which are most favourably exposed in areas of

458   extensive rock outcrop, rather than abundant spoil debris (Davies and Shillito, 2018, 2021;

459   Shillito and Davies, 2020).

460   No trace fossils are thus far known from the Northumberland Basin, but the Stainmore

461   Formation is directly contemporaneous in age, and comparable in facies, with the Upper

462   Limestone Formation of the adjacent Midland Valley Basin of southern Scotland. Despite

463   different lithostratigraphic and basin names, the units were deposited within a linked

464   deposystem during the Pendleian, connected by contiguous deltaic sedimentary environments

465   in the present North Sea area, with upland and emergent areas in the region of the Southern

466   Uplands Block (Figure 2) (Kearsey et al., 2015, 2019). *Diplichnites cuithensis* trackways are

467   common in the Upper Limestone Formation, recorded from both Glasgow city, 170 km WNW

468   (Buckman, pers. comm), and the Isle of Arran, 220 km WNW (Figure 12; the type locality of

469   *D. cuithensis*; Briggs et al., 1979). Marginally older, Visean, strata of the Midland Valley basin

470   in Fife (Anstruther and Pittenweem formations) also have abundant reported *D. cuithensis*

471   (Pearson, 1992; Whyte, 2018) and original fieldwork at these localities has yielded 26

472   individual instances of the track form, ranging in external width from 23-47 cm (mean 32 cm),

473   and indented into sand to depths of up to 8 mm. These dimensions strongly suggest that the

474   trackways were made by organisms of the same size and posited weight as recorded by the

475   Howick body fossil. The trackways all occur in similar sedimentary facies to the Howick body

476   fossil – delta top alluvial and littoral sandstone facies with patchy standing tree fossils and

477   abundant *Stigmaria*, but no evidence for extensive afforestation. They provide direct evidence

478   for arthropleurid habitat preferences, with individual trackways traversing both submerged and

479 emergent substrates (Figure 12). This ichnological evidence supports physiological evidence

480 that arthropleurids were suited to both subaerial and very shallow water locomotion (e.g.,

481 Størmer, 1976; Shear and Selden, 1995; Schneider and Barthel, 1997), and would have been

482 well-suited to the patchily wet lower delta plain environment recorded in the Howick section.

483 *Palaeogeographic and stratigraphic range*

484 The full known stratigraphic and palaeogeographic range of arthropleurids is shown in Figure

485 13 and Table 1. The organism is known from Visean to Sakmarian aged strata and has a tight

486 palaeogeographic range in the narrow equatorial belt (Schneider and Werneburg, 2010).

487 *Distribution of* Arthropleura *fossil sites*

488 The earliest fossil evidence is known from a handful of Mississippian sites in Britain and

489 Germany (including this study) and becomes widespread across equatorial Euramerica later in

490 the Carboniferous. Peak geographic distribution of unequivocal body and trace fossils is known

491 from the Early to Middle Pennsylvanian. Post-Kasimovian body fossils are less common, with

492 evidence primarily from a few sites in central and southern Europe (Table 1), despite a notably

493 abundant trackway record from this interval across North America (Ryan, 1986; Ryan and

494 Boehner, 1994; Mángano et al., 2002; Lucas et al., 2005; Martino and Greb, 2009; Schneider

495 et al., 2010; Chaney et al., 2013). Two secondary reports of fragmentary remains and trackways

496 from Kazakhstan (Novozhylov, 1962; Nelikhov, 2010), recently cited by Dernov (2019),

497 would represent a higher latitude palaeogeographic outlier, but these instances remain

498 anecdotal in the absence of published illustration, and the host strata are only coarsely dated to

499 the Pennsylvanian.

500 The shifting distribution of both body and trace fossil evidence for *Arthropleura* (Figure 13)

501 may imply that the palaeogeographic range of arthropleurids expanded from a localized

502 subequatorial crucible in the Middle to Late Mississippian. The fossil described here, in

503 addition to the Scottish trackways, indicates Mississippian gigantism in this group, before

504 arthropleurid fossils become widespread in the late Carboniferous. By the Pennsylvanian,

505 *Arthropleura* had an extensive west-east palaeogeographic range across the entire continent of

506 Laurussia/Pangea, but no verified evidence for the organism is present from palaeolatitudes

507 higher than 10° north or south, and most known instances tightly follow the palaeoequator

508 (Schneider and Werneburg 2010, fig. 16). In the Late Pennsylvanian and early Permian, a

509 transcontinental range was maintained, but almost all known arthropleurid and track instances

510 remain within 10° of the palaeoequator. The Carboniferous-Permian northwards drift of Pangea

511 appears to be reflected by the increased abundance of younger *Arthropleura* remains from more

512 southern modern latitudes, as fossil evidence tracks the relative southwards migration of the

513 palaeoequator during this interval.

514 The strong relationship between *Arthropleura* body fossils and the location of the

515 palaeoequator could be counter-argued to be reflective of sampling biases, tracking the

516 distribution of mined coal-bearing strata. However, the trend is also seen within the trace fossil

517 record (Figure 13), which is subject to a different and mutually exclusive suite of biases (i.e.,

518 extensive bedding plane outcrop, instead of excavated spoil tips). For example, in Britain,

519 multiple outcrops of strata with bedding plane exposures persist through the latest

520 Carboniferous and early Permian and have been investigated for (vertebrate) trackways (e.g.,

521 Sarjeant, 1974; Hedge et al., 2019); yet, despite these directed ichnological surveys and the

522 correct outcrop type, the youngest British trace fossil evidence for *D. cuithensis* is

523 Serpukhovian (Briggs et al., 1979). By contrast, in Spain, the oldest worked coal measures are

524 of Moscovian age (Piedad-Sánchez et al., 2004) and spoil from these measures has been

525 intensively interrogated for plant and other fossil remains (e.g., Wagner and Álvarez-Vázquez,

526 2010); yet, despite these directed palaeontological surveys and the correct outcrop type, the

527 earliest Spanish body fossil evidence for *Arthropleura* is not known until the Kasimovian

528   (Castro, 1997). These examples illustrate that while different outcrop expressions can bias

529   evidence for *Arthropleura*, the appearance and disappearance of suitable outcrop types is

530   discordant with the appearance and disappearance of evidence for *Arthropleura.* The most

531   parsimonious explanation for the southwards drift of evidence through the Carboniferous and

532   Permian is that the affinity of *Arthropleura* for equatorial latitudes was robust, and that the

533   genus maintained its geographic range as the Carboniferous continents drifted northwards.

534   *Response to Carboniferous-Permian climate change and oxygen*

535   The undisrupted record of *Arthropleura* throughout the interval of the Kasimovian rainforest

536   collapse (DiMichele et al., 2009, 2011; Sahney et al., 2010; Davies and Gibling, 2011; Falcon-

537   Lang et al., 2018; Bashforth et al., 2021) is testament to the fact that the organism was not

538   reliant on wetland coal forests as a habitat. The increasing post-Kasimovian dominance of

539   seasonally dry vegetation and open forests in equatorial Euramerica (DiMichele, 2014) appears

540   to have had little impact on the palaeogeographic range and abundance of evidence for

541   *Arthropleura*. However, increasing aridity during Pangean assembly may explain changes in

542   evidence of arthropleurids. The post-Kasimovian record of *Arthropleura* shows a shift where

543   trace fossil sites become almost as abundant as those yielding cuticular fossils. While

544   *Arthropleura* appears to have successfully weathered climate and habitat change around the

545   Carboniferous-Permian boundary, the youngest evidence for the organism is known from the

546   Sakmarian of Saxony, Germany (Rößler et al., 2012). The absence of records younger than c.

547   290 Ma despite fossils of other terrestrial fauna suggests that the early Permian disappearance

548   of *Arthropleura* records the extinction of the organism. The reason for this extinction may be

549   related to increasing supercontinental aridification near the equator, in addition to increased

550   competition associated with the Permian rise of reptiles (Schneider et al. 2010).

551 The age of giant *Arthropleura* is frequently linked to atmospheric oxygen peaks, which are

552 suggested to have facilitated gigantism (e.g., Harrison et al., 2010; Vermeij, 2016; McGhee,

553 2018). If atmospheric oxygen is not the primary constraint on arthropod body size, however,

554 ecological interactions with predators, environmental factors, and Cope's Rule are alternative

555 potential drivers (e.g., Hone and Benton, 2004; Schneider and Werneburg, 2010; Schachat et

556 al., 2018). The known stratigraphic range of *Arthropleura* is discordant with the Palaeozoic

557 oxygen peaks predicted by the GEOCARBSULF model (Berner et al., 2006), with the first

558 appearance of *Arthropleura* (and other giant aquatic and terrestrial arthropods; Carpenter,

559 1939; Braddy et al. 2008) pre-dating significant rises in atmospheric O_2, and the last appearance

560 of trace or body fossil evidence for *Arthropleura* pre-dating the oxygen peak of the mid-

561 Permian). The Howick specimen dates from an interval when atmospheric O_2 was not

562 significantly elevated above the present day, at 23% (Berner et al., 2006), and suggests that

563 high atmospheric oxygen concentrations alone were not required for the evolution of a 2.63 m

564 long myriapod, c. 50 kg in weight. Hence a more parsimonious explanation for the gigantism

565 of this organism was that it evolved and sustained giant dimensions simply due a favourable

566 environment with a limited number of competitors (e.g., the anthracosaur tetrapods recorded

567 by *Baropezia*), few predators, and an abundance of high-nutrition food (potentially including

568 prey (Schneider et al., 2010; Schneider and Werneburg (2010)).

569 **CONCLUSIONS**

570 Recently discovered giant arthropleurid remains in the Serpukhovian Stainmore Formation of

571 the Northumberland Basin are notable because they constitute one of the largest known

572 arthropod fossils in the world, are presently the remains of the largest individual arthropod

573 known to have evolved and are the oldest semi-complete body fossil evidence for gigantism in

574 arthropleurids. The fossil is also notable taphonomically as the individual is partially three-

575 dimensionally preserved, interred in sand, and was deformed by syn-sedimentary tectonics

576 prior to lithification. The specimen is interpreted as the anterior part of an exuvium, which

577 sedimentological evidence suggests was discarded on the banks of a small coastal river

578 channel, where it sat amongst plant detritus and filled with sand through open sutures, before

579 being entrained and interred in the channel by bank collapse.

580 The fossil and its context lend weight to recent assertions about arthropleurids: they lived in

581 open wooded habitats, instead of, or in preference to, the coal forests with which they have

582 traditionally been associated; they occupied the same environmental niches as early tetrapods;

583 they were highly manoeuvrable; and they had hardened sclerotized cuticle. The

584 Northumberland specimen has much in common with the 59 other body and trace fossil records

585 of *Arthropleura* from Visean to Sakmarian strata from equatorial Euramerica. This fossil

586 presents a rare example of the remains of this giant millipede, up to 2.63 metres long and c. 50

587 kg in weight, the likes of which crawled throughout the Earth's equatorial region for a ~45

588 million year interval of the late Palaeozoic.

REFERENCES

Allport, H.A., Davies, N.S., Shillito, A.P., Mitchell, E.G., and Herron, S.T., 2021. Non-palimpsested crowded *Skolithos* ichnofabrics in a Carboniferous tidal rhythmite: disentangling ecological signatures from the spatio-temporal bias of outcrop. Sedimentology. https://doi.org/10.1111/sed.12947

Almond J.E. 1985. Les Arthropleurides du Stéphanien de Montceau-les-Mines, France. Bulletin de la Société d'Histoire Naturelle d'Autun. 115, pp.59–60.

623   Anderson, L.I., Dunlop, J.A., Horrocks, C.A., Winkelmann, H.M. and Eagar, R.M.C., 1997.

624   Exceptionally preserved fossils from Bickershaw, Lancashire UK (Upper Carboniferous,

625   Westphalian A (Langsettian)). Geological Journal, 32(3), pp.197-210.

626   Andrée, K., 1913. Weiteres über das carbonische Arthostraken-Genus Arthopleura Jordan.

627   Palaeontographica, (A) 60, pp. 295-310.

628   Bashforth, A.R., DiMichele, W., Eble, C.F., Falcon-Lang, H., Looy, C., and Lucas, S.G., 2021.

629   The environmental implications of upper Paleozoic plant-fossil assemblages with mixtures of

630   wetland and drought-tolerant taxa in tropical Pangea. Geobios, 68, pp.1-15.

631   https://doi.org/10.1016/j.geobios.2021.04.002

632   Braddy, S.J., Poschmann, M. and Tetlie O.E., 2008. Giant claw reveals the largest ever

633   arthropod. *Biology Letters*, 4(1), pp.106–109.

634   Bailey, L.W., 1902, Report upon the Carboniferous system of New Brunswick with special

635   reference to workable coal. Geological Survey of Canada. No. 799, in Annual Report, Volume

636   XIII, 1900 Geological Survey of Canada No. 830 (1903), pp. 1M–38M.

637   Bercovitz, K. and Warburg, M.R., 1985. Developmental patterns in two populations of the

638   millipede *Archispirostreptus syriacus* (De Saussure) in Israel (Diplopoda). Bijdragen tot de

639   Dierkunde, 55(1), pp.37-46.

640   Berner, R.A., 2006. GEOCARBSULF: a combined model for Phanerozoic atmospheric O2 and

641   CO2. Geochimica et Cosmochimica Acta, 70(23), pp.5653-5664.

642   Booth, M.G., Underhill, J.R., Gardiner, A. and McLean, D., 2020. Sedimentary and tectonic

643   controls on Lower Carboniferous (Visean) mixed carbonate–siliciclastic deposition in NE

644   England and the Southern North Sea: implications for reservoir architecture. Petroleum

645   Geoscience, 26(2), pp.204-231.

646 Boule M. 1893. Sur les débris d'*Arthropleura* trouvés en France. Bulletin de la Société de

647 l'Industrie Minérale, (3), 7, pp. 619-638.

648 Boyd, C. and McIlroy, D., 2016. Three-dimensional morphology and palaeobiology of the trace

649 fossil *Dactyloidites jordii* nov. isp. from the Carboniferous of England. Geobios, 49(4), pp.257-

650 264.

651 Boyd, C. and McIlroy, D., 2017. Three-dimensional morphology of *Beaconites capronus* from

652 Northeast England. Ichnos, 24(4), pp.250-258.

653 Boyd, C. and McIlroy, D., 2018. The morphology and mode of formation of *Neoeione* igen.

654 nov. from the Carboniferous of northern England. Paläontologische Zeitschrift, 92(1), pp.179-

655 190.

656 Braddy, S.J., Poschmann, M. and Tetlie, O.E., 2008. Giant claw reveals the largest ever

657 arthropod. Biology Letters, 4(1), pp.106-109.

658 Brauckmann, C., Gröning, E. and Thiele-Bourcier, M., 1997. Kopf-und Schwanz-Region von

659 *Arthropleura* armata Jordan, 1854 (Arthropoda; Ober-Karbon). Geologica et Palaeontologica,

660 31(1), pp.79-92.

661 Briggs, D.E.G., 1986. Walking trails of the giant arthropod *Arthropleura*. Bulletin trimestriel

662 de la Société d'histoire naturelle et des amis du Muséum d'Autun, (117), pp.141-147.

663 Briggs, D.E.G. & Almond, J.E., 1994. The arthropleurids from the Stephanian (Late

664 Carboniferous) of Montceau-les-Mines (Massif Central - France). In: Poplin, C. & Heyler, D.

665 (Eds.), Quand le Massif Central était sous l'équateur: un écosystème Carbonifère à Montceau-

666 les-Mines. Mémoires de la Section des Sciences, 12, pp. 127-135.

667 Briggs, D.E.G., Rolfe, W.D.I. and Brannan, J., 1979. A giant myriapod trail from the Namurian

668 of Arran, Scotland. Palaeontology, 22(2), pp.273-291.

669   Briggs, D.E.G., Plint, A.G. and Pickerill, R.K., 1984. *Arthropleura* trails from the Westphalian

670   of eastern Canada. Palaeontology, 27(4), pp.843-855.

671   Briggs, D.E.G., Stankiewicz, B.A., Meischner, D., Bierstedt, A. and Evershed, R.P., 1998.

672   Taphonomy of arthropod cuticles from Pliocene lake sediments, Willershausen, Germany.

673   Palaios, 13(4), pp.386-394.

674   Burt, T. and Tucker, M., 2020. The Geomorphology of the Whin Sill. In: Goudie, A., Migon,

675   P. (eds.) Landscapes and Landforms of England and Wales (pp. 515-530). Springer, Cham.

676   Calder, J., Rygel, M., Ryan, R., Falcon-Lang, H. and Herbert, B., 2005. Stratigraphy and

677   sedimentology of early Pennsylvanian red beds at Lower Cove, Nova Scotia, Canada: the Little

678   River Formation with redefinition of the Joggins Formation. Atlantic Geology, 41(2-3),

679   pp.143-167.

680   Calman, W.T., 1914. III.—On *Arthropleura* Moyseyi, n. sp., from the Coal-Measures of

681   Debyshire. Geological Magazine, 1(12), pp.541-544.

682   Carpenter, F.M., 1939. The Lower Permian Insects of Kansas. Part 8: Additional

683   Megasecoptera, Protodonata, Odonata, Homoptera, Psocoptera, Protelytroptera, Plectoptera

684   and Protoperlaria. *Proceedings of the American Academy of Arts and Sciences* 73(3), pp.29-

685   70.

686   Castro, M.P., 1997. Hallazgos de" *Arthropleura*" en el Estefaniense de la Península Ibérica.

687   Revista española de paleontología, 12(1), pp.15-22.

688   Chadwick, R.A., Holliday, D.W., Holloway, S., and Hulbert, A.G., 1995. The structure and

689   evolution of the Northumberland-Solway Basin and adjacent areas. Subsurface Memoir of the

690   British Geological Survey, HM Stationery Office, 109 pp.

691   Chaney D.S., Lucas S.G., and Elrick S. 2013. New occurrence of an arthropleurid trackway

692   from the lower Permian of Utah. In: Lucas S.G., DiMichele W.A., Barrick J.E., Schneider J.W.,

693   Spielmann J.A., editors. The Carboniferous–Permian transition. Vol. 60. Albuquerque: New

694   Mexico Museum of Natural History and Science; pp.64–65.

695   Cohen, K.M., Finney, S.C., Gibbard, P.L., and Fan, J.-X., 2021 (2013; updated). The ICS

696   International Chronostratigraphic Chart v. 2021/07. Episodes 36: pp.199-204.

697   http://www.stratigraphy.org/ICSchart/ChronostratChart2021-07.pdf

698   Cózar, P. and Somerville, I.D., 2012. The Carboniferous Archerbeck Borehole, near Canonbie

699   (Dumfriesshire, southern Scotland): biostratigraphic revision of the late Asbian to early

700   Pendleian succession using foraminiferans and regional correlations. Earth and Environmental

701   Science Transactions of the Royal Society of Edinburgh, 103(1), pp.105-122.

702   Cózar, P. and Somerville, I.D., 2020. Foraminiferal biostratigraphy of Brigantian-Arnsbergian

703   limestones from eastern Scotland and Northumberland (northeast England). Earth and

704   Environmental Science Transactions of The Royal Society of Edinburgh, pp.1-15.

705   Cózar, P. and Somerville, I.D., 2021. The Serpukhovian in Britain: use of foraminiferal

706   assemblages for dating and correlating. Journal of the Geological Society, 178 (3): jgs2020-

707   170.

708   Davies, N.S. and Gibling, M.R., 2011. Evolution of fixed-channel alluvial plains in response

709   to Carboniferous vegetation. Nature Geoscience, 4(9), pp.629-633.

710   Davies, N.S. and Gibling, M.R., 2013. The sedimentary record of Carboniferous rivers:

711   continuing influence of land plant evolution on alluvial processes and Palaeozoic ecosystems.

712   Earth-Science Reviews, 120, pp.40-79.

713   Davies, N.S. and Shillito, A.P., 2018. Incomplete but intricately detailed: The inevitable
714   preservation of true substrates in a time-deficient stratigraphic record. Geology, 46(8), pp. 679-
715   682.

716   Davies, N.S. and Shillito, A.P., 2021. True substrates: the exceptional resolution and
717   unexceptional preservation of deep time snapshots on bedding surfaces. Sedimentology.
718   https://doi.org/10.1111/sed.12900

719   Dean, M.T., Browne, M.A.E., Waters, C.N. and Powell, J.H., 2011. A lithostratigraphical
720   framework for the Carboniferous successions of northern Great Britain (onshore). British
721   Geological Survey Research Report RR/10/07.

722   De La Comble, J., 1963. Un arthropode encore inconnu du Permien, *Arthropleura* spec.
723   Bulletin de la Société d'Histoire Naturelle d'Autun. Autun, 28, p. 6.

724   De Paola, N., Holdsworth, R.E., McCaffrey, K.J. and Barchi, M.R., 2005. Partitioned
725   transtension: an alternative to basin inversion models. Journal of Structural Geology, 27(4), pp.
726   607-625.

727   Dernov, V., 2019. Taphonomy and paleoecology of fauna and flora from deltaic sandstones of
728   Mospinka Formation (Middle Carboniferous) of Donets Basin. Geo&Bio, 18, pp. 37-63.

729   DiMichele, W.A., Hook, R.W., Beerbower, R., Boy, J.A., Gastaldo, R.A., Hotton III, N.,
730   Phillips, T.L., Scheckler, S.E., Shear, W.A. and Sues, H.D., 1992. Paleozoic terrestrial
731   ecosystems. In: Behrensmeyer, A.K., Damuth, J.D., DiMichele, W.A., Potts, R., Sues, H.-D.,
732   and Wing, S.L., (eds.) Terrestrial ecosystems through time. University of Chicago Press,
733   Chicago, pp.205-325.

734   DiMichele, W.A., Montañez, I.P., Poulsen, C.J. and Tabor, N.J., 2009. Climate and
735   vegetational regime shifts in the late Paleozoic ice age earth. Geobiology, 7(2), pp. 200-226.

736   DiMichele, W.A., Cecil, C.B., Chaney, D.S., Elrich, S.D., Lucas, S.G., Lupia, R., Nelson, W.J.,

737   and Tabor, N.J., 2011. Pennsylvanian-Permian vegetational changes in tropical Euramerica.

738   In: Harper, J.A. (Ed.), Geology of the Pennsylvanian-Permian in the Dunkard Basin.

739   Guidebook, 76th Annual Field Conference of Pennsylvania Geologists, Washington, pp. 60–

740   102.

741   DiMichele, W.A., 2014. Wetland-dryland vegetational dynamics in the Pennsylvanian ice age

742   tropics. International Journal of Plant Sciences, 175(2), pp.123-164.

743   Donovan, S.K., 2002. Arthropleurid myriapods. Geology Today, 18(1), pp.35-37.

744   Elliott, T., 1976. Sedimentary sequences from the Upper Limestone Group of Northumberland.

745   Scottish Journal of Geology, 12(2), pp.115-124.

746   Falcon-Lang, H.J., Benton, M.J., Braddy, S.J., and Davies, S.J., 2006, The Pennsylvanian

747   tropical biome reconstructed from the Joggins Formation of Nova Scotia, Canada: Journal of

748   the Geological Society, London, v. 163, pp. 561–576,

749   Falcon-Lang, H.J. and Miller, R.F., 2007. Palaeoenvironments and palaeoecology of the Early

750   Pennsylvanian Lancaster Formation ('Fern Ledges') of Saint John, New Brunswick, Canada.

751   Journal of the Geological Society, 164(5), pp.945-957.

752   Falcon-Lang, H.J., Minter, N.J., Bashforth, A.R., Gibling, M.R. and Miller, R.F., 2015. Mid-

753   Carboniferous diversification of continental ecosystems inferred from trace fossil suites in the

754   Tynemouth Creek Formation of New Brunswick, Canada. Palaeogeography,

755   Palaeoclimatology, Palaeoecology, 440, pp.142-160.

756   Falcon-Lang, H.J., Nelson, W.J., Heckel, P.H., DiMichele, W.A., and Elrick, S.D., 2018. New

757   insights on the stepwise collapse of the Carboniferous Coal Forests: Evidence from cyclothems

758 and coniferopsid tree-stumps near the Desmoinesian–Missourian boundary in Peoria County,

759 Illinois, USA. Palaeogeography, Palaeoclimatology, Palaeoecology, 490, pp. 375–392.

760 Farmer, N. and Jones, J.M., 1969. The Carboniferous Namurian rocks of the coast section from

761 Howick Bay to Foxton Hall, Northumberland. Transactions of the Natural History Society of

762 Northumberland, 17, pp.1-27.

763 Farmer, N., Jones, J.M. and Murchison, D.G., 1970. The identity of the Lickar Limestone of

764 north Northumberland and its underlying coals. Scottish Journal of Geology, 6(2), pp.200-207.

765 Ferguson, L., 1966. The recovery of some large track-bearing slabs from Joggins, Nova Scotia.

766 Atlantic Geology, 2, pp.128-130.

767 Frank, M.C. and Tyson, R.V., 1995. Parasequence-scale organic facies variations through an

768 early Carboniferous Yoredale cyclothem, Middle Limestone Group, Scremerston,

769 Northumberland. Journal of the geological Society, 152(1), pp.41-50.

770 Fraser, A.J. and Gawthorpe, R.L., 2003. An atlas of Carboniferous basin evolution in northern

771 England. Geological Society, London, Memoir 28, 79pp.

772 Garwood, R. and Dunlop, J., 2014. The walking dead: Blender as a tool for paleontologists

773 with a case study on extinct arachnids. Journal of Paleontology, 88(4), pp.735-746.

774 Getty, P., Sproule, R., Stimson, M. and Lyons, P., 2017. Invertebrate trace fossils from the

775 Pennsylvanian Rhode Island formation of Massachusetts, USA. Atlantic Geology, 53, pp.185-

776 206.

777 Greb, S.F., DiMichele, W. A. and Gastaldo, R.A., 2006. Evolution and importance of wetlands

778 in earth history. Geological Society of America Special Paper 399, 42 pp.

779 Guthörl, P., 1934. Die Arthropoden aus dem Carbon und Perm des Saar-Nahe-Pfalz-Gebietes.

780 Abhandlungen der Preussischen Geologischen Landesanstalt, Neue Folge 164: pp.1-219

781 Guthörl P. 1935. Entdeckung und Bergung des größten, bis jetzt bekannten Exemplars von

782 *Arthropleura armata* Jordan & v. Meyer in Grube Maybach-Saar. Zeitschrift der Deutschen

783 Geologischen Gesellschaft, 87, pp. 687–692.

784 Guthörl P. 1936. *Arthropleura*, der Riesengliederfüßler des Oberkarbons, und seine

785 Verbreitung in den europäischen Steinkohlenbecken. Glückauf. 39: pp.965–976.

786 Guthörl, P. 1940. Zur Arthropoden-Fauna des Karbons und Perms. 12. Insekten- und

787 *Arthropleura*-Reste aus der Tiefbohrung 38 (Hangard) bei Neunkirchen-Saar. -

788 Paläontologische Zeitschrift, 22, pp. 109-119.

789 Hahn, G., Hahn, R. and Brauckmann, C., 1986. Zur Kenntnis von *Arthropleura* (Myriapoda;

790 Ober-Karbon). Geologica et Palaeontologica, (20), pp.125-137.

791 Hannibal, J.T., 1997. Remains of *Arthropleura*, a gigantic myriapod arthropod, from the

792 Pennsylvanian of Ohio and Pennsylvania. Kirtlandia, 50, pp. 1-9.

793 Harrison, J.F., Kaiser, A. and Van den Brooks, J.M., 2010. Atmospheric oxygen level and the

794 evolution of insect body size. Proceedings of the Royal Society B: Biological Sciences,

795 277(1690), pp.1937-1946.

796 Heckel, P.H. and Clayton, G., 2006. Use of the new official names for the subsystems, series

797 and stages of the Carboniferous System in international journals. Proceedings of the Geologists'

798 Association, 4(117), pp.393-396.

799 Hedge, J., Shillito, A.P., Davies, N.S., Butler, R.J. and Sansom, I.J., 2019. Invertebrate trace

800 fossils from the Alveley member, Salop Formation (Pennsylvanian, Carboniferous),

801 Shropshire, UK. Proceedings of the Geologists' Association, 130(1), pp.103-111.

802 Hone, D.W. and Benton, M.J., 2005. The evolution of large size: how does Cope's Rule work?.

803 Trends in Ecology & Evolution, 20(1), pp.4-6.

804   Horváthová, T., Šustr, V., Chroňáková, A., Semanová, S., Lang, K., Dietrich, C., Hubáček, T.,

805   Ardestani, M.M., Lara, A.C., Brune, A. and Šimek, M., 2021. Methanogenesis in the digestive

806   tract of the tropical millipedes *Archispirostreptus gigas* (Diplopoda, Spirostreptidae) and

807   *Epibolus pulchripes* (Diplopoda, Pachybolidae). Applied and Environmental Microbiology,

808   pp.AEM-00614.

809   Ingrams, S., McLean, D., Booth, M. and Bodman, D.J., 2020. Biostratigraphy and

810   paleoecology of Asbian–Brigantian (Mississippian) miospores from Berwick-upon-Tweed,

811   Northumberland, UK: Preliminary results. Review of Palaeobotany and Palynology, p.104206.

812   Jordan F.W.H. and von Meyer H. 1854. Über die Crustaceen der Steinkohlenformation von

813   Saarbrücken. Palaeontographica. 4, 1–15.

814   Kearsey, T., Ellen, R., Millward, D. and Monaghan, A.A.. 2015 Devonian and Carboniferous

815   stratigraphical correlation and interpretation in the Central North Sea, Quadrants 25 – 44.

816   Energy and Marine Geoscience Programme Commissioned Report CR/15/117. British

817   Geological Survey, 80 pp.

818   Kearsey, T.I., Millward, D., Ellen, R., Whitbread, K. and Monaghan, A.A., 2019. Revised

819   stratigraphic framework of pre-Westphalian Carboniferous petroleum system elements from

820   the Outer Moray Firth to the Silverpit Basin, North Sea, UK. Geological Society, London,

821   Special Publications, 471(1), pp.91-113.

822   Kimbell, G.S., Chadwick, R.A., Holliday, D.W. and Werngren, O.C., 1989. The structure and

823   evolution of the Northumberland Trough from new seismic reflection data and its bearing on

824   modes of continental extension. Journal of the Geological Society, 146(5), pp.775-787.

825   Kjemperud, M.V., 2011. Fault architecture of reactivated faults in Carboniferous sediments,

826   Northumberland, Great Britain (Master's thesis, University of Oslo).

827   Kraus O, Brauckmann C. 2003. Fossil giants and surviving dwarfs. Arthropleurida and

828   Pselaphognatha (Atelocerata, Diplopoda): characters, phylogenetic relationships and

829   construction. Verhandlungen des naturwissenschaftlichen Vereins in Hamburg, 40, 5–50.

830   Kraus, W. 1993. Eine 2 m lange semiflexible Rekonstruktion von *Arthropleura*, dem größten

831   bekannten Myriapoden aus dem Oberkarbon Mitteleuropas. Der Präparator, 39, 141–158.

832   Langiaux J, Sotty D. 1977. Ichnologie 4: pistes et empreintes dans le Stéphanien de Blanzy-

833   Montceau. La Physiophile, 86, 74–91.

834   Latreille P.A. 1802. Histoire naturelle générale et particulière des crustacés et des insectes:

835   ouvrage faisant suite aux Oeuvres de Leclerc de Buffon, et partie du Cours complet d'histoire

836   naturelle rédigé par C.S. Sonnini, 7. 413 pp. F. Dufart, Paris.

837   Leeder, M.R., Fairhead, D., Lee, A., Stuart, G. and Clemmey, H., 1989. Sedimentary and

838   tectonic evolution of the Northumberland Basin. In: Arthurton, R.J., Gutteridge, P. and Nolan,

839   S.C. (eds) The role of tectonics in Devonian and Carboniferous sedimentation in the British

840   Isles. Yorkshire Geological Society Occasional Publication, 6, 207–223.

841   Lucas, S.G., Lerner, A.J., Hannibal, J.T., Hunt, A.P. and Schneider, J.W., 2005. Trackway of

842   a giant *Arthropleura* from the Upper Pennsylvanian of El Cobre Canyon, New Mexico. In

843   Geology of the Chana Basin. New Mexico Geological Society, 56th Field Conference

844   Guidebook, pp. 279-282.

845   Mángano, M.G., Buatois, L.A., West, R.R., Maples, C.G., 2002. Ichnology of a Pennsylvanian

846   equatorial tidal flat: the Stull Shale Member at Waverly, eastern Kansas. Kansas Geological

847   Survey Bulletin, 245, 133 p.

848   Martino, R.L. and Greb, S.F., 2009. Walking trails of the giant terrestrial arthropod

849   *Arthropleura* from the Upper Carboniferous of Kentucky. Journal of Paleontology, 83(1),

850   pp.140-146.

851   McCoy, V.E. and Brandt, D.S., 2009. Scorpion taphonomy: criteria for distinguishing fossil

852   scorpion molts and carcasses. The Journal of Arachnology, 37(3), pp.312-320.

853   McGhee Jr, G.R., 2018. Carboniferous Giants and Mass Extinction: The Late Paleozoic Ice

854   Age World. Columbia University Press.

855   Minter, N.J., Buatois, L.A., Mángano, M.G., Davies, N.S., Gibling, M.R. and Labandeira, C.,

856   2016. The establishment of continental ecosystems. In Buatois, L.A., Mángano, M.G., (eds.)

857   The Trace-Fossil Record of Major Evolutionary Events (pp. 205-324). Springer, Dordrecht.

858   Moreau, J.D., Gand, G., Fara, E., Galtier, J., Aubert, N. and Fouché, S., 2019. Trackways of

859   *Arthropleura* from the Late Pennsylvanian of Graissessac (Hérault, southern France).

860   Historical Biology, pp.1-12.

861   Mwabvu, T., Hamer, M., Slotow, R.O.B. and Barraclough, D., 2010. A revision of the

862   taxonomy and distribution of *Archispirostreptus* Silvestri 1895 (Diplopoda, Spirostreptida,

863   Spirostreptidae), and description of a new spirostreptid genus with three new species. Zootaxa,

864   2567(1), pp.1-49.

865   Nelikhov, A., 2010. In the dungeons of Dzhezkazgan. PaleoMir, 1 (8): 60–69. Available at:

866   http://iae.makorzh.ru/Tchudinov/Nelikhov1/index.htm

867   Novozhylov, N., 1962. Family Arthropleuridae Zittel, 1848. In: Rodendorf B.B. (Ed.).

868   Fundamentals of paleontology. Arthropods. Tracheata and Chelicerata. Publishing House of

869   the Academy of Sciences of the USSR, Moscow, 25.

870   Pacyna, G., Florjan, S. and Borzęcki, R., 2012. New morphological features of *Arthropleura*

871   sp. (Myriapoda, Diplopoda) based on new specimens from the Upper Carboniferous of Lower

872   Silesia (Poland). Annales Societatis Geologorum Poloniae, 82, pp. 121-126.

873   Pavela M., 2018. Fossil species from the Carboniferous: *Arthropleura* Jordan & Meyer 1854.

874   PALEO 2018:74. Available at: https://www.paleontology.cz/clanky/arthropleura.html

875   Pearson, P.N., 1992. Walking traces of the giant myriapod *Arthropleura* from the Strathclyde

876   Group (Lower Carboniferous) of Fife. Scottish Journal of Geology, 28(2), pp.127-133.

877   Pearson, P.N. and Gooday, R.J., 2019. A large *Taenidium* burrow from the Upper

878   Carboniferous of Corrie, Isle of Arran, and remarks on the association of *Taenidium* burrows

879   and *Diplichnites* trails. Scottish Journal of Geology, 55(2), pp.135-140.

880   Perrier, V. and Charbonnier, S., 2014. The Montceau-les-Mines Lagerstätte (Late

881   Carboniferous, France). Comptes Rendus Palevol, 13(5), pp.353-367.

882   Piedad-Sánchez, N., Suárez-Ruiz, I., Martínez, L., Izart, A., Elie, M. and Keravis, D., 2004.

883   Organic petrology and geochemistry of the Carboniferous coal seams from the Central Asturian

884   Coal Basin (NW Spain). International Journal of Coal Geology, 57(3-4), pp.211-242.

885   Pillola, G.L. and Zoboli, D., 2021. First occurrence of *Arthropleura armata* (Myriapoda) in the

886   Moscovian (Carboniferous) of SW Sardinia (Italy). Bollettino della Società Paleontologica

887   Italiana, 60, pp. 1-6, doi:10.4435/BSPI.2021.01.

888   Proctor, C.J., 1998. Arthropleurids from the Westphalian D of Writhlington Geological Nature

889   Reserve, Somerset. Proceedings of the Geologists' Association, 109(2), pp.93-98.

890   Pruvost, P., 1930. La faune continentale du terrain houiller de la Belgique. Memoires du Musee

891   royal d'histoire naturelle de Belgique, 44, pp. 103–282.

892 Reynolds, A.D., 1992. Storm, wave and tide-dominated sedimentation in the Dinantian Middle

893 Limestone Group, Northumbrian Basin. Proceedings of the Yorkshire Geological Society,

894 49(2), pp.135-148.

895 Richards, B.C., 2013. Current status of the international Carboniferous time scale. The

896 Carboniferous-Permian Transition, New Mexico Museum of Natural History and Science

897 Bulletin, 60, pp.348-353.

898 Richardson, E.S., 1959. Pennsylvanian invertebrates of the Mazon Creek area, Illinois;

899 Trilobitomorpha, Arthropleurida II. Fieldana: Geology, 12, pp. 79–82.

900 Rolfe, W.I. and Ingham, J.K., 1967. Limb structure, affinity and diet of the Carboniferous

901 'centipede'*Arthropleura*. Scottish Journal of Geology, 3(1), pp.118-124.

902 Rößler, R. and Scheider, J.W., 1997, Eine bemerkenswerte Paläobiocoenose im Unterkarbon

903 Middeleuropastt – Fossilführung und Paläoenvironment der Hainichen-Subgruppe

904 (Erzgebirge-Becken). Veröffentlichungen des Museum für Naturkunde Chemnitz, 20, pp.5-44.

905 Rößler, R., Zierold, T., Feng, Z., Kretzschmar, R., Merbitz, M., Annacker, V. and Schneider,

906 J.W., 2012. A snapshot of an early Permian ecosystem preserved by explosive volcanism: new

907 results from the Chemnitz petrified forest, Germany. Palaios, 27(11), pp.814-834.

908 Rudkin, D.M., Young, G.A., Elias, R.J. and Dobrzanski, E.P., 2003. The world's biggest

909 trilobite—*Isotelus rex* new species from the Upper Ordovician of northern Manitoba, Canada.

910 Journal of Paleontology, 77(1), pp.99-112.

911 Ryan, R., 1986. Fossil myriapod trails in the Permo-Carboniferous strata of northern Nova

912 Scotia, Canada. Atlantic Geology, 22(2), pp.156-161.

913 Ryan, R.J. and Boehner, R.C., 1994, Geology of the Cumberland Basin, Cumberland,

914 Colchester and Pictou Counties, Nova Scotia. Nova Scotia Department of Natural Resources,

915 Mines and Energy Branches, Mem., 10, 222 pp.

916 Sahney, S., Benton, M.J. and Falcon-Lang, H.J., 2010. Rainforest collapse triggered

917 Carboniferous tetrapod diversification in Euramerica. Geology, 38(12), pp.1079-1082.

918 Salter, J.W., 1863. On some species of Eurypterus and allied forms. Quarterly Journal of the

919 Geological Society, 19(1-2), pp.81-87.

920 Sarjeant, W.A.S., 1974. A history and bibliography of the study of fossil vertebrate footprints

921 in the British Isles. Palaeogeography, Palaeoclimatology, Palaeoecology, 16(4), pp.265-378.

922 Scarboro, D.D. and Tucker, M.E., 1995. Amphibian footprints from the mid-Carboniferous of

923 Northumberland, England: sedimentological context, preservation and significance.

924 Palaeogeography, Palaeoclimatology, Palaeoecology, 113(2-4), pp.335-349.

925 Schachat, S.R., Labandeira, C.C., Saltzman, M.R., Cramer, B.D., Payne, J.L. and Boyce, C.K.,

926 2018. Phanerozoic p O2 and the early evolution of terrestrial animals. Proceedings of the Royal

927 Society B: Biological Sciences, 285(1871), p.20172631.

928 Schneider, J. and Barthel, M., 1997. Eine Taphocoenose mit *Arthropleura* (Arthropoda) aus

929 dem Rotliegend (? Unterperm) des Döhlen-Becken (Elbe-Zone, Sachsen). Freiberger

930 Forschungsheft, C 466, pp.183-223.

931 Schneider, J.W. and Werneburg, R., 1998. *Arthropleura* und Diplopoda (Arthropoda) aus dem

932 Unter-Rotliegend (Unter-Perm, Assel) des Thüringer Waldes (Südwest-Saale-Senke).

933 Veröffentlichungen Naturhistorisches Museum Schleusingen, 13, pp.19-36.

934 Schneider, J.W., Lucas, S.G., Werneburg, R. and Rößler, R., 2010. Euramerican Late

935 Pennsylvanian/Early Permian arthropleurid/tetrapod associations–implications for the habitat

936 and paleobiology of the largest terrestrial arthropod. Carboniferous–Permian transition in

937 Canon del Cobre, northern New Mexico. Edited by Lucas SG, Schneider JW, Spielmann J.

938 New Mexico Museum of Natural History and Science, Bulletin, 49, pp.49-70.

939 Schneider, J.W. and Werneburg, R., 2010. *Arthropleura*, der größte landlebende Arthropode

940 der Erdgeschichte – neue Funde und neue Ideen.- Semana, 25, pp. 75-100.,

941 Scott, A.C. and Taylor, T.N., 1983. Plant/animal interactions during the Upper Carboniferous.

942 The Botanical Review, 49(3), pp.259-307.

943 Shear, W.A. and Edgecombe, G.D., 2010. The geological record and phylogeny of the

944 Myriapoda. Arthropod Structure & Development, 39(2-3), pp.174-190.

945 Shear, W. and Selden, P., 1995. *Eoarthropleura* (Arthropoda, Arthropleurida) from the Silurian

946 of Britain and the Devonian of North America. Neues Jahrbuch für Geologie und

947 Paläontologie-Abhandlungen, pp.347-375.

948 Sheppard, T.H., 2005. A stratigraphical framework for the Upper Langsettian and

949 Duckmantian of the East Pennine Coalfields. British Geological Survey, 20pp. (IR/05/070)

950 Shillito, A.P. and Davies, N.S., 2020. The Tumblagooda Sandstone revisited: exceptionally

951 abundant trace fossils and geological outcrop provide a window onto Palaeozoic littoral

952 habitats before invertebrate terrestrialization. Geological Magazine, 157(12), pp.1939-1970.

953 Śtamberg, S. and Zajíc, J., 2008. Carboniferous and Permian faunas and their occurrence in the

954 limnic basins of the Czech Republic. Museum of Eastern Bohemia at Hradec Kralové, 224 p.

955 Størmer, L., 1976. Arthropods from the Lower Devonian (Lower Emsian) of Alken an der

956 Mosel, Germany. 5. Myriapoda and additional forms, with general remarks on fauna and

957 problems regarding invasion of land by arthropods. Senckenbergiana Lethaea, 51(4), pp.335-

958 59.

959 Torsvik, T.H. and Cocks, L.R.M., 2016. Earth history and palaeogeography. Cambridge

960 University Press.

961 Tucker, M.E., Gallagher, J. and Leng, M.J., 2009. Are beds in shelf carbonates millennial-scale

962 cycles? An example from the mid-Carboniferous of northern England…. Sedimentary

963 Geology, 214(1-4), pp.19-34.

964 Turner, N. and Spinner, E., 1992. Palynological evidence for the early Namurian age of the

965 "Millstone Grit" and Upper Limestone Group around Longhoughton Steel, Northumberland.

966 Proceedings of the Yorkshire Geological Society, 49(1), pp.11-22.

967 Vermeij, G.J., 2016. Gigantism and its implications for the history of life. PLoS One, 11(1),

968 p.e0146092.

969 Vernon, R.D., 1912. On the geology and palaeontology of the Warwickshire Coalfield.

970 Quarterly Journal of the Geological Society, 68(1-4), pp.587-638

971 Von Siebold, C.T., 1848. Lehrbuch der vergleichenden Anatomie der Wirbellosen Thiere.

972 Erster Theil. In: von Siebold C.T. & Stannius H. (eds.), Lehrbuch der vergleichenden

973 Anatomie. – Verlag von Veit & Comp., Berlin. 679 pp

974 Von Zittel, K.A., 1885. Handbuch der Palaeontologie: Abtheilung 1, Palaeozoologie -

975 Mollusca und Arthropoda, 2. 893 pp. R. Oldenbourg, München.

976 Wagner, R.H. and Álvarez-Vázquez, C., 2010. The Carboniferous floras of the Iberian

977 Peninsula: a synthesis with geological connotations. Review of Palaeobotany and Palynology,

978 162(3), pp.239-324.

979 Waterlot, G. 1934. Étude de la faune continentale du terrain houiller sarrolorrain: Étude des

980 Gites minéraux de la France. Bassin houiller de la Sarre et de la Lorraine 2, Faune fossile. 320

981 pp. L. Daniel, Lille.

982 Waters, C.N., Millward, D. and Thomas, C.W., 2014. The Millstone Grit group

983 (Pennsylvanian) of the Northumberland–Solway Basin and Alston Block of northern England.

984 Proceedings of the Yorkshire Geological Society, 60(1), pp.29-51.

985 Westoll, T.S., Robson, D.A. and Green, R., 1955. A guide to the geology of the district around

986 Alnwick, Northumberland. Proceedings of the Yorkshire Geological Society, 30(1), pp.61-100.

987 Whyte, M.A., 2018. Mating trackways of a fossil giant millipede. Scottish Journal of Geology,

988 54(1), pp.63-68.

989 Wilson, H.M., 1999. Palaeobiology of the Arthropleuridea. PhD Thesis, The University of

990 Manchester. Available at: https://ethos.bl.uk/OrderDetails.do?uin=uk.bl.ethos.536226

991 Woodward, H., 1907. Further Notes on the Arthropoda of the British Coal-Measures.

992 Geological Magazine, 4(12), pp.539-549.

993 **FIGURE CAPTIONS**

994 Figure 1 – Specimen of partial remains of a giant *Arthropleura* (anterior 12-14 tergites) after

995 excavation from the Serpukhovian Stainmore Formation, Howick Bay, Northumberland,

996 England (CAMSM X.50355). Part A and Part B are not true part and counterpart but rather a

997 split through the middle of a three-dimensional dorsal exoskeleton (see Fig. 7 and discussion

998 in text).

999 Figure 2 – Interpreted sketch of the fossil, as preserved in Slab A, whilst still intact in fallen

1000 block of host sandstone prior to excavation. The overlap-pattern of the paratergites on the left

1001 indicate, that this is the ventral site of the dorsal exoskeleton. Therefore, the typical

1002 ornamentation of the dorsal site of *Arthropleura* tergites and paratergites is not visible.

1003 Figure 3 – Geological context of the site. A) Locality within the Northumberland Basin. B)

1004 Geological map of the fossil locality. C) Regional stratigraphy. D) Sedimentary log of the fossil

1005   site. E) Structural profile along cliffs at southern end of Howick Bay, showing fossil site within

1006   damage zone of the Howick Fault (location of section denoted with British National Grid

1007   references).

1008   Figure 4 – Context of the specimen prior to extraction. A) Part A of the fossil (facing

1009   stratigraphically downwards). Note convex-up doming of host sediment. Scale bar is 20 cm

1010   long. Ruler is 20 cm. B) Part B of the fossil (facing stratigraphically-upwards). C) The fallen

1011   block in which the fossil was discovered in January 2018 (white circle), showing split in rock

1012   where fossil was exposed (white triangle). Black circle denotes position in cliff profile from

1013   where the block fell. Listric faults in hanging wall of Howick Fault are highlighted, exhibiting

1014   hanging wall thickening of mudrock (HT), attesting to syn-sedimentary origin (red arrows

1015   indicate sense of fault movement). Scale bar is 2 metres. D) View of the fallen block (white

1016   circle) and original position (black circle) in the context of the Howick Fault damage zone and

1017   master fault separating the Alston and Stainmore formations (HT is at same position as in C).

1018   Host bed is immediately adjacent to one of two syn-sedimentary (Mississippian) normal faults

1019   that were later reactivated as strike-slip faults during the latest Carboniferous to Permian

1020   emplacement of the Whin Sill dolerite intrusion (De Paola et al., 2005). This structural context

1021   attests to strain in the fossil-bearing sandstone bed prior to full lithification and may explain

1022   certain features of the fossil (see main text). Blue dashed line signifies approximate

1023   stratigraphic position of the Lickar Limestone, marking the onset of the late Serpukhovian

1024   (Cózar and Somerville, 2021). Scale bar is 5 metres. Photograph in D courtesy of Geospatial

1025   Research Limited.

1026   Figure 5 – Sedimentological characteristics of the Stainmore Formation at the southern end of

1027   Howick Bay, attesting to lower delta plain deposition. A) Rotated view of fallen block hosting

1028   fossil at starred horizon, showing lithology of amalgamated trough cross beds of fine sandstone,

1029   coarsening upwards from laminated very fine sandstone and siltstone. Located at c. 8-10

metres on stratigraphic log in Fig. 3D. Scale bar is 20 cm. B) Casts of syneresis cracks on

underside of fallen block. Located at 8 metres on stratigraphic log in Fig. 3D. Scale bar is 10

cm. C) Detail of cross-bedded sets in which *Arthropleura* fossil was interred. Note clasts of

coaly debris. Located at 9.5 metres on stratigraphic log in Fig. 3D. Ruler is 20 cm. D) Crudely

developed rhythmites of probable tidal origin, colonized with *Skolithos* (Sk) and *Teichnichnus*

(Te) burrows. Located at 6 metres on stratigraphic log in Fig. 3D. Scale bar is 15 cm. E)

Inclined heterolithic stratification in form of lateral accretion (LA) set of small tidal channel;

northwards direction of migration arrowed. Located at 1.5 metres on stratigraphic log in Fig.

3D. Scale bar is 70 cm. F) Incised channel filled with braided alluvium and cutting into

underlying sequence at far southern end of Howick Bay. Approximate channel base

highlighted. Channel truncates sequence illustrated in Fig. 3D. Scale bar is 2 m.

Figure 6 – Ichnological and palaeobotanical features associated with the *Arthropleura* fossil.

A) Trackway of an anthracosaur tetrapod (*Baropezia*) (individual footprints arrowed). Located

at 4.6 metres on stratigraphic log in Fig. 3D. Scale bar is 10 cm. B) Detail of *Baropezia* footprint

(*Ba*), adjacent to *Stigmaria* root (black arrow). For details of vertebrate tracks prior to recent

erosional degradation, see Scarboro and Tucker (1995). Located at 4.6 metres on stratigraphic

log in Fig. 3D. Scale bar is 20 cm. C) Thinly bedded wave rippled facies immediately below

fossil horizon, exhibiting horizontal invertebrate burrows *Planolites* (Pl) and *Archaeonassa*

(Ar). Located at 10.6 metres on stratigraphic log in Fig. 3D. Scale bar is 10 cm. D) Tightly

curved invertebrate burrow identified as *Taenidium* due to meniscate fill and absence of lining.

Fallen block of same lithology adjacent to fossil-bearing block. Scale bar is 10 cm. E) Ripple-

laminated sandstone beds colonized with coalified, downwards-branching plant rootlets.

Located at 9.0 metres on stratigraphic log in Fig. 3D. Scale bar is 20 cm. F) Plant remains in

same bed as *Arthropleura* fossil, including fragment of branch or bark belonging to

Lepidodendron sensu lato (black arrow) and thin axis that acutely bifurcates distally, possibly

being the proximal part of a medullosalean pteridosperm frond (white arrow). Located at 10.0 metres on stratigraphic log in Fig. 3D. Scale bar is 20 cm. G) Seed fossils, possibly *Samaropsis*, as produced by cordaitaleans. Note seeds occur immediately adjacent to the *Arthropleura* remains in the part, seen at top left of image. Located at 10.2 metres on stratigraphic log in Fig. 3D. Scale bar is 5 cm. H) *Stigmaria* on stratigraphic base of fallen block hosting the *Arthropleura* remains. Preserved fraction of main rhizomorph axis extends between white arrows and exhibits ornamentation in boxed area. Adjacent part of bedding plane contains traces of rootlets (r) branching from the main rhizomorph. Located at 9.8 metres on stratigraphic log in Fig. 3D Scale bar is 1 metre.

Figure 7 – Cartoon diagram illustrating taphonomic context and relationship between key attributes of the specimen.

Figure 8 – Details of the *Arthropleura* specimen. A) Alternation of granular (1) and smooth (2) texture on medial tergites. Granular texture interpreted to reflect degraded verrucose texture to anterior part of each tergite. View of underside of dorsal exoskeleton preserved on surface of Slab A. Scale bar is 1 cm. B) Detail of right lateral paratergites seen on Slab B, exhibiting striated patterning and frayed margins to the paratergites. Scale bar is 1 cm. C) Micaceous and carbonaceous smear on fragment of upper side of dorsal exoskeleton (Slab A). Scale bar is 1 cm. D) Inflection of paratergites (1) relative to medial tergites (2) at anterior of specimen on the part. Head region seen at (3). Scale bar is 1 cm. E) Detail of invertebrate burrow (*Planolites*) seen in centre of Slab B, and likely exploiting remains shortly after interment. Scale bar is 1 cm.

Figure 9 – Three-dimensional morphology of cuticular sand infill preserved in Slab A. A-B) Images of Slab A before and after extraction of fossil. A shows natural break in sandstone revealing underside of dorsal cuticle, notable for carbonaceous material (cb) between

1079 paratergites and presence of granular texture. B shows Slab A after extraction, revealing cast

1080 of the dorsal exoskeleton, still yielding carbonaceous material but with no granular texture.

1081 Scale bar is 20 cm. C-D) Images of partial fragment of cuticular sand infill between the

1082 underside and upperside of the dorsal cuticle, as extracted from Slab A. C shows exoskeleton

1083 underside with granular texture, and both images show cross-section through lenticular

1084 imbricated tergites, possibly compressed by synsedimentary tectonics. (An = anterior; Po =

1085 posterior). Scale bar is 1 cm.

1086 Figure 10 – Detail of Slab A (A-B) and Slab B (C-D) with interpreted sketches of margins

1087 showing offset of three dimensional sand infill from carbonaceous smear. Same tergites on

1088 each slab are colour coded (with reference to prominent tergite shown in white). Cuticular

1089 interior shown as full circles with correspondingly shaped carbonaceous smear shown as colour

1090 coded partial circles, indicating consistent 40 cm squeezed offset of infill from cuticle in

1091 direction of red bidirectional arrow, associated with synsedimentary deformation. Scale bar is

1092 20 cm.

1093 Figure 11 –Reconstruction of the Howick specimen shown to scale relative to other known

1094 evidence of *Arthropleura*. A) Reconstructions of *Arthropleura* from the three articulated giant

1095 specimens (preserved remains highlighted pink). B) Largest *Diplichnites cuithensis* trackways

1096 known from each Carboniferous stage, shown at same scale as reconstructions in A. Note that

1097 previously known partially complete body fossils were both markedly smaller than the

1098 dimensions of *Arthropleura* revealed by trace fossil evidence. For references and details of

1099 localities mentioned see Table 1.

1100 Figure 12 – Trace fossil evidence for *Arthropleura* from the trackway *Diplichnites cuithensis*,

1101 preserved in strata, near contemporaneous in age to the Howick specimen, from adjacent basins

1102 in northern Britain (see Figure 3 for localities). A) Trackway from which the *D. cuithensis*

1103   holotype was cast (Briggs et al., 1979) in the Serpukhovian Limestone Coal Formation of

1104   Laggan, Isle of Arran, Scotland. Stick is one metre long, inner and outer width of trackway

1105   highlighted. B) *D. cuithensis* trackway of near-analogous width to the Howick body fossil,

1106   Visean Pittenweem Formation, Crail, Fife, Scotland. C) *D. cuithensis* trackway more than 10

1107   metres long (arrowed) in the Visean Pittenweem Formation, St. Andrews, Fife, Scotland (see

1108   Whyte, 2018). Geologist is 1.8 metres tall. D-E) Photograph and interpreted sketch of context

1109   of *D. cuithensis* on a true substrate (Davies and Shillito, 2018, 2021) recording passage of two

1110   animals between emergent and subaqueous substrates. Convex bedform, colonized with plants,

1111   provided small island surrounded by shallow water puddles in a delta top setting. Trackways

1112   are well-defined on emergent substrate and less so on subaqueous parts of substrate. Visean

1113   Anstruther Formation, 3.5 km northwest of Kingsbarns, Fife, Scotland. Measuring stick is 60

1114   cm long.

1115   Figure 13 – Palaeogeographic range of *Arthropleura* body and trace fossils. A) Known sites of

1116   evidence plotted on a palaeogeographic map of the late Carboniferous (c. 310 Ma; after Torsvik

1117   and Cocks, 2017). Numbers refer to sites listed in Table 1. B-D) Distribution of sites by age,

1118   shown relative to position of palaeoequator (red) and 10° latitude (pink). B) Visean to

1119   Serpukhovian sites (latitudinal parallels shown for c. 320 Ma, from Torsvik and Cocks, 2017).

1120   C) Bashkirian to Moscovian sites (latitudinal parallels shown for c. 310 Ma, from Torsvik and

1121   Cocks, 2017). D) Kasimovian to Sakmarian sites (latitudinal parallels shown for c. 290 Ma,

1122   from Torsvik and Cocks, 2017).

1123   Table 1 – Details of previously reported *Arthropleura* localities.

table 1   Click here to access/download;table;REV Table 1 1121.xlsx ⬇

Number	Age	Stratigraphic context
1	Serpukhovian	Stainmore Formation
2	Moscovian	Sulzbach Formation
3	Gzhelian-Asselian	Döhlen Formation
4	Gzhelian-Asselain	Montceau-les-Mines lägerstatten
5	Bashkirian	Pennine Middle Coal Measures Formation
6	Visean	Berthelsdorf Formation
7	Serpukhovian	Lower Silesian Basin
8	Serpukhovian	Upper Silesian Basin
9	Pennsylvanian	Karaganda Basin
10	Bashkirian	Charleroi Formation
11	Bashkirian	Grand Anse Formation
12	Bashkirian	Joggins Formation
13	Bashkirian	Lancaster Formation
14	Bashkirian	Mospinka Formation
15	Bashkirian	Nord-Pas-de-Calais Mining Basin
16	Bashkirian	Pennine Lower Coal Measures Formation
17	Bashkirian	Pennine Middle Coal Measures Formation
18	Bashkirian	Pennine Middle Coal Measures Formation
19	Bashkirian	Upper Silesian Basin
20	Bashkirian	Žacleř Formation
21	Bashkirian-Moscovian	Emma mine
22	Moscovian	Francis Creek Shale
23	Moscovian	Grovesend Formation
24	Moscovian	Heiligenwald Formation
25	Moscovian	Kittaning Formation
26	Moscovian	Lorraine basin
27	Moscovian	Pennine Middle Coal Measures Formation
28	Moscovian	Plzeň Basin
29	Bashkirian	Ruda Beds
30	Moscovian	Saarbrücker Subgroup
31	Moscovian	San Giorgio Formation
32	Moscovian	Scottish Upper Coal Measures Formation
33	Kasimovian	Conemaugh Formation
34	Kasimovian	Kateřina Coal Mine
35	Kasimovian	San José Formation
36	Gzhelian	La Magdalena Coalfield
37	Gzhelian	Stephanian strata
38	Gzhelian	Stephanian strata
39	Gzhelian	Toledo Mountains
40	Asselian	Manebach Formation
41	Asselian	Autunian strata
42	Sakmarian	Leukersdorf Formation
43	Visean	Anstruther and Pittenweem formations
44	Serpukhovian	Limestone Coal Formation
45	Serpukhovian	Limestone Coal Formation
46	Pennsylvanian	Zhezkazgan Group
47	Bashkirian	Boss Point Formation
48	Bashkirian	Little River and Joggins formations
49	Bashkirian	Mospinka Formation

50	Bashkirian	Tynemouth Creek Formation
51	Moscovian	Malagash Formation
52	Moscovian	Rhode Island Formation
53	Kasimovian	Cutler Group
54	Gzhelian	Cape John Formation
55	Gzhelian	Conemaugh Formation
56	Gzhelian	Eiche Member (Flechtingen Formation)
57	Gzhelian	Graissessac Formation
58	Gzhelian-Asselian	Montceau Formation
59	Gzhelian	Stull Shale Member (Kanwaka Formation)
60	Asselian	Halgaito Formation

Location	Type
Howick, Northumberland, England	Giant partial
Maybach mine, Saarland, Germany	Giant partial
Döhlen Basin, Saxony, Germany	Giant partial
Montceau-les-Mines, Burgundy, France	Small complete
Shipley, Derbyshire, England	Small partial
Hainichen Basin, Saxony, Germany	Fragmentary remains
Przygorze - KWK Boleslaw, Poland	Fragmentary remains
Chlebovice - Důl Staříč, Czech Republic	Fragmentary remains
Karaganda, Kazakhstan	Fragmentary remains
Mariemont mine, Hainaut, Belgium	Fragmentary remains
Maringouin, New Brunswick, Canada	Fragmentary remains
Joggins, Nova Scotia, Canada	Fragmentary remains
Saint John, New Brunswick, Canada	Fragmentary remains
Makedonovka, Donets Basin, Ukraine	Fragmentary remains
Anzin, Hauts-de-France, France	Fragmentary remains
Bickershaw, Lancashire, England	Fragmentary remains
Barnsley, Yorkshire, England	Fragmentary remains
Baxterley, Warwickshire, England	Fragmentary remains
Czerwionka - Ameryka, Poland	Fragmentary remains
Nowa Ruda, Lower Silesia, Poland	Fragmentary remains
Brunssum, Limburg, Netherlands	Fragmentary remains
Mazon Creek, Illinois, USA	Fragmentary remains
Camerton & Writhlington, Somerset, England	Fragmentary remains
Friedrichsthal, Saarland, Germany	Fragmentary remains
Cannelton, Pennsylvania, USA	Fragmentary remains
St. Avold, Grand Est, France	Fragmentary remains
Salford, Lancashire, England	Fragmentary remains
Zbůch - Důl Austria, Czech Republic	Fragmentary remains
Chwałowice, Lower Silesia, Poland	Fragmentary remains
Saarbrücken region, Saarland, Germany	Fragmentary remains
Rio San Giorgio, Sardinia, Italy	Fragmentary remains
Leven, Fife, Scotland	Fragmentary remains
Columbiana County, Ohio, USA	Fragmentary remains
Radvanice, Ostrava, Czech Republic	Fragmentary remains
Ciñera, León, Spain	Fragmentary remains
Carrocera, León, Spain	Fragmentary remains
St. Etienne, Auvergne-Rhône-Alpes, France	Fragmentary remains
Commentry, Auvergne-Rhône-Alpes, France	Fragmentary remains
Puertollano, Ciudad Real, Spain	Fragmentary remains
Manebach, Thuringia, Germany	Fragmentary remains
Autun, Burgundy, France	Fragmentary remains
Chemnitz, Saxony, Germany	Fragmentary remains
Crail to St. Andrews, Fife, Scotland	Multiple trackways
Isle of Arran, Scotland	Single trackway
Glasgow, Scotland	Single trackway
Zhezkazgan, Kazakhstan	Single trackway
Alma, New Brunswick, Canada	Single trackway
Joggins, Nova Scotia, Canada	Multiple trackways
Makedonovka, Donets Basin, Ukraine	Multiple trackways

Gardner Creek, New Brunswick, Canada	Multiple trackways
Pugwash to Smith Point, Nova Scotia, Canada	Multiple trackways
Plainville, Massachusetts, USA	Multiple trackways
El Cobre Canyon, New Mexico, USA	Single trackway
Cape John, Nova Scotia, Canada	Multiple trackways
Boyd County, Kentucky, USA	Multiple trackways
Flechtingen Volcanic Complex, Germany	Multiple trackways
Graissessac, Hérault, France	Multiple trackways
Montceau-les-Mines, Burgundy, France	Multiple trackways
Waverly, Kansas, USA	Multiple trackways
Lime Ridge, Utah, USA	Single trackway

Reference

This study
Guthörl (1934, 1935); Hahn et al. (1986); Kraus and Brauckmann (2003); Kraus (2005)
Schneider & Barthel (1997); Schneider et al. (2010)
Briggs & Almond (1984); Almond (1985); Perrier & Charbonnier (2014)
Calman (1914); Hahn et al. (1986)
Rößler & Schneider (1997); Schneider et al (2010)
Pavela (2018)
Pavela (2018)
Novozhylov (1962); Dernov (2019)
Pruvost (1930)
R. Miller (pers. comm.: New Brunswick Museum specimen NBMG15084)
Falcon-Lang et al. (2006)
Falcon-Lang and Miller (2007)
Dernov (2019)
Pruvost (1930)
Anderson et al. (1997)
Andrée (1913)
Vernon (1912); Pruvost (1930)
Pavela (2018)
Pacyna et al (2012); Pavela (2018)
Pruvost (1930)
Richardson (1959); Hannibal (1997)
Woodward (1907); Andrée (1913); Proctor (1998)
Jordan (1854)
Hannibal (1997)
Waterlot (1934)
Salter (1863); Pruvost (1930), Hahn et al., (1986)
Pavela (2018)
Andrée (1913)
Andrée (1913)
Pillola & Ziboli (2021)
Andrée (1913)
Hannibal (1997)
Stamberg & Zajic (2008)
Castro (1997)
Castro (1997)
Boule (1893), Waterlot (1934)
Boule (1893)
Castro (1997)
Schneider & Werneberg (1998)
de La Comble (1963); Moreau et al (2019)
Rößler et al (2012)
Pearson (1992); Whyte (2018)
Briggs et al. (1979)
J. Buckman (pers. com.)
Nelikhov (2010); Dernov (2019)
Bailey (1902)
Ferguson (1966); Calder et al (2005); Falcon-Lang et al (2006)
Dernov (2019)

Briggs et al. (1984); Falcon-Lang et al. (2015)
Ryan (1986); Ryan & Boehner (1994)
Getty et al. (2017)
Lucas et al. (2005); Schneider et al. (2010)
Ryan (1986); Ryan & Boehner (1994)
Martino & Greb (2009)
Walter & Gaitzsch (1988); Schneider & Werneburg (2010)
Moreau et al. (2019)
Langiaux & Sotty (1977); Briggs (1986)
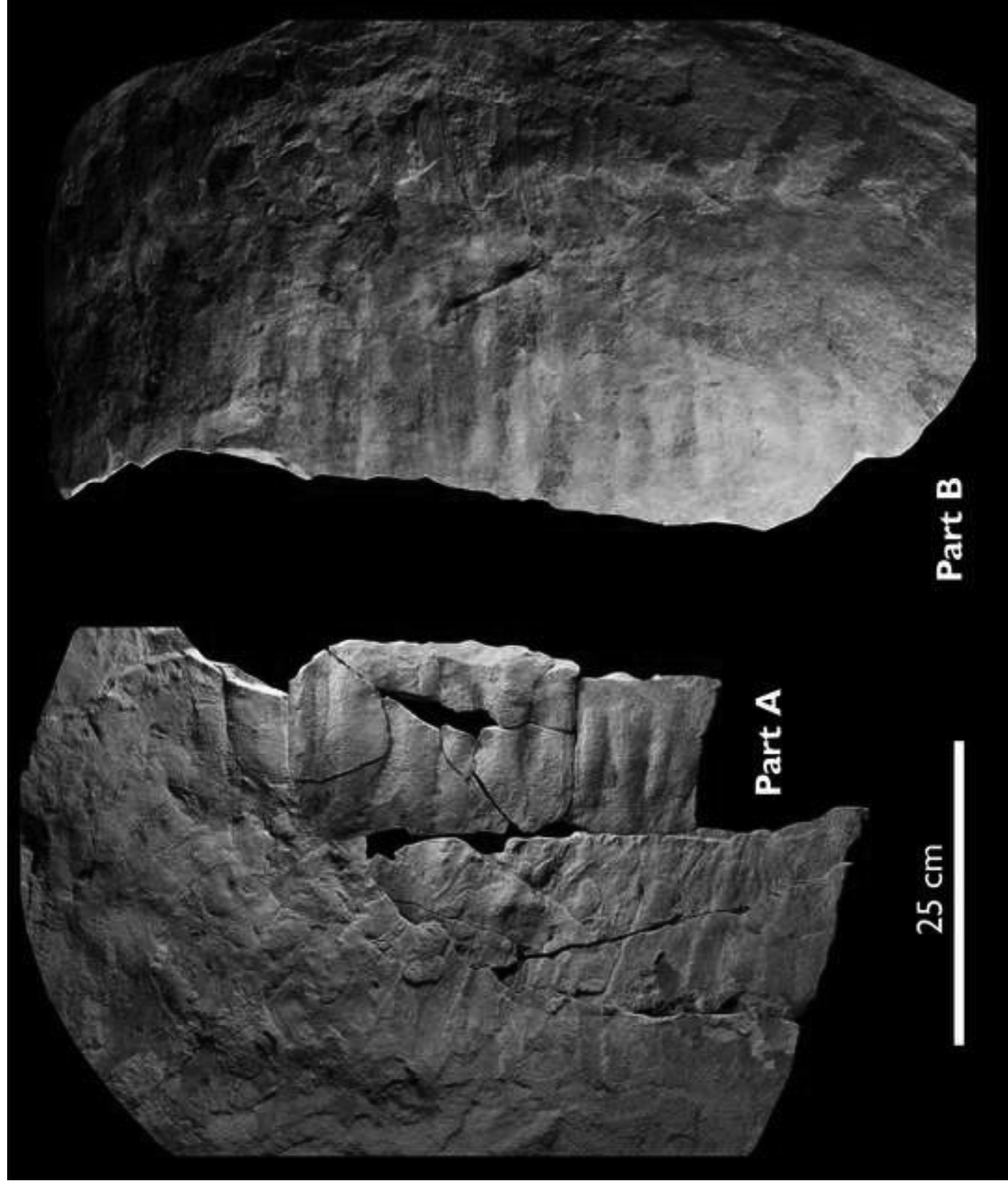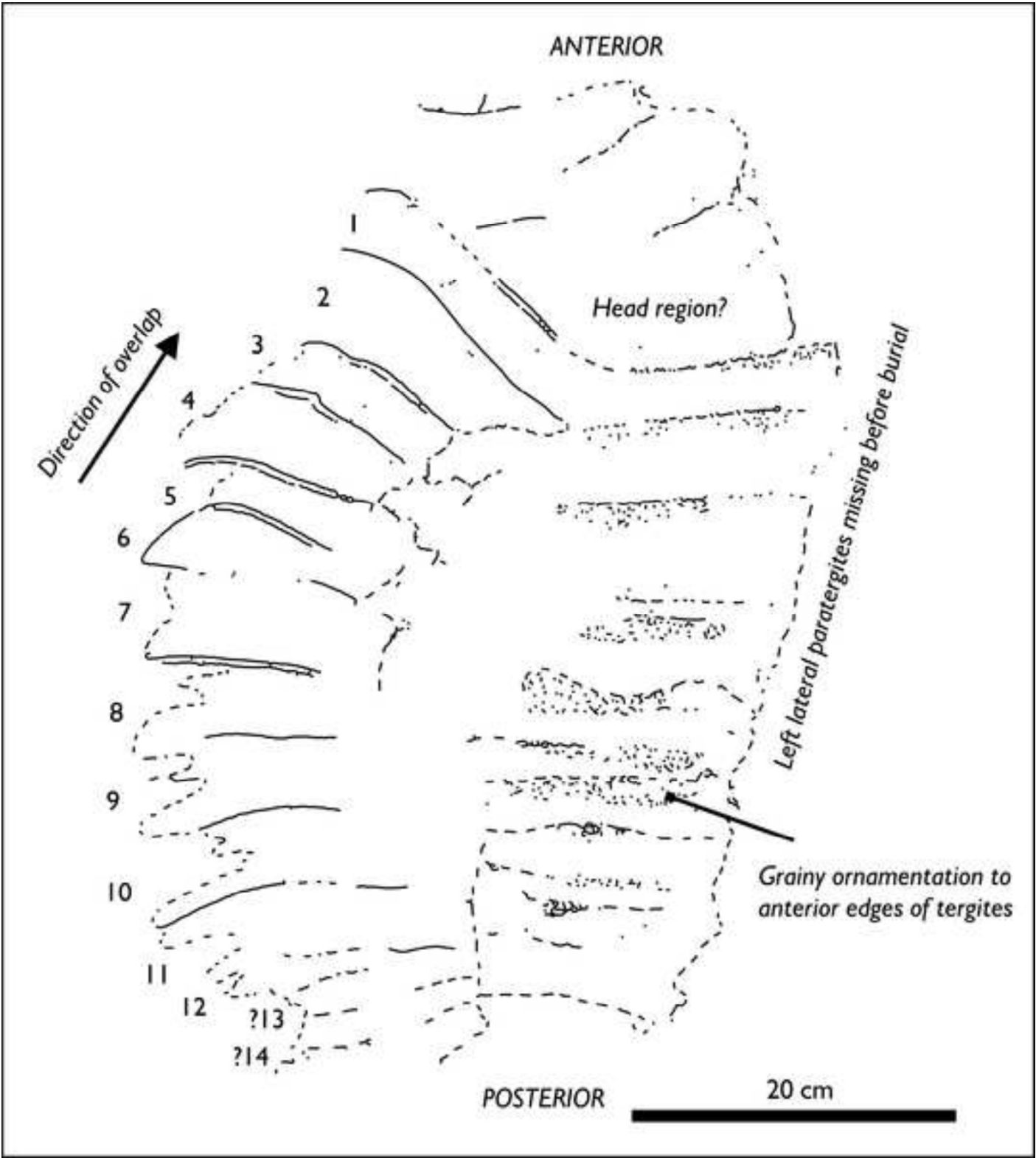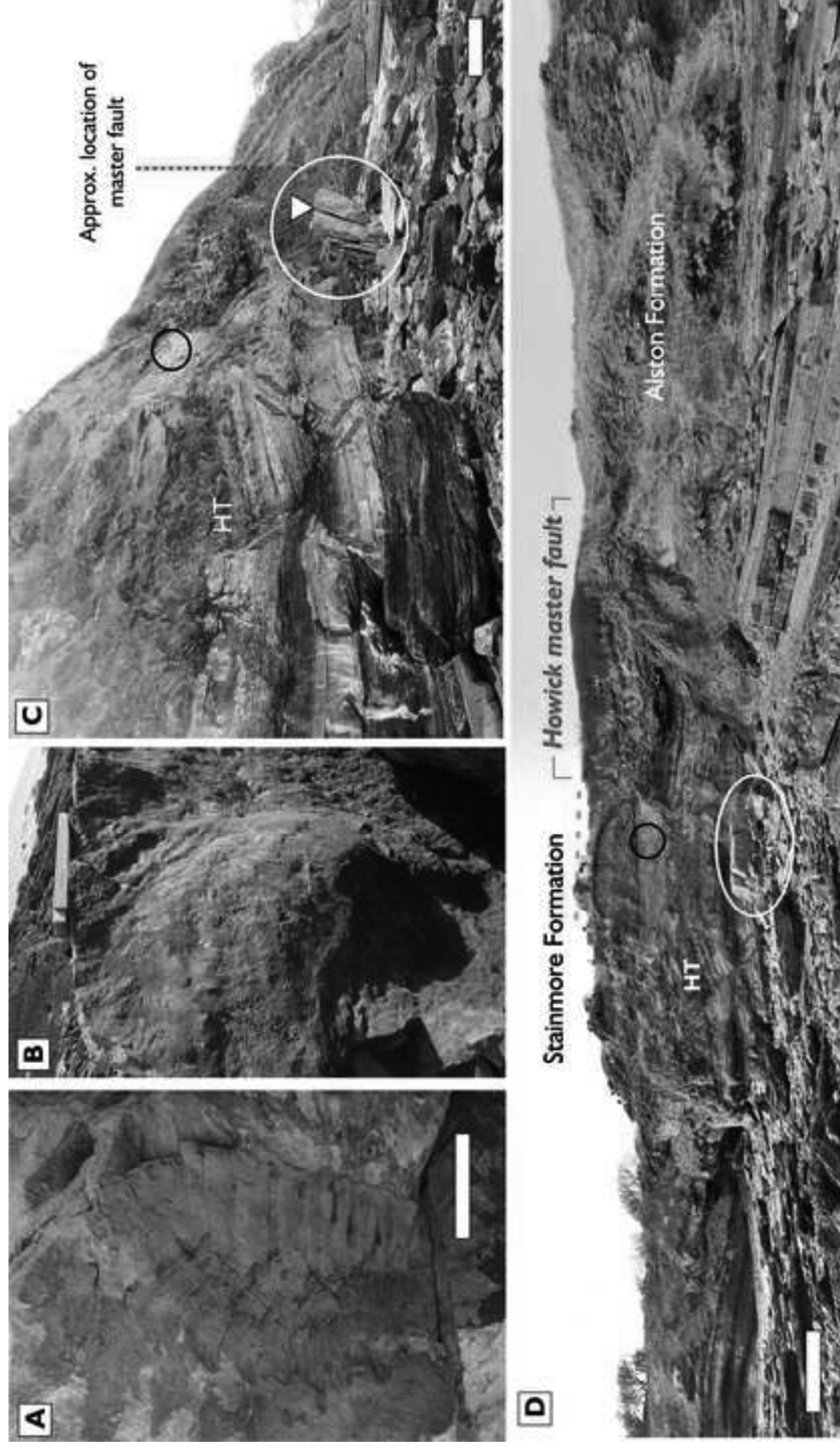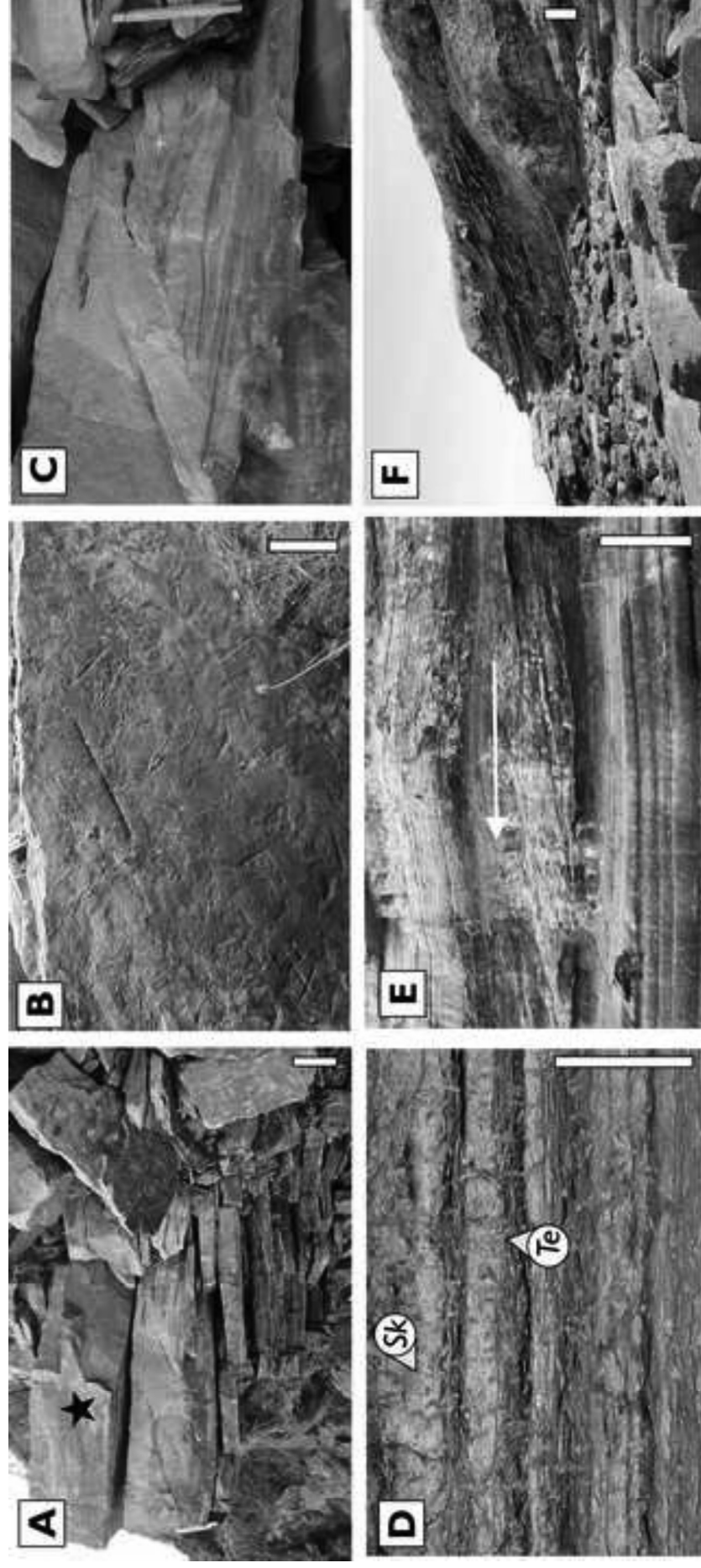Mángano et al. (2002)
Chaney et al. (2013)

figure 1

Part A

Part B

25 cm

figure 2

Click here to access/download;figure;Art resub F2.jpg ⬇

ANTERIOR

1

2

Head region?

3

Direction of overlap

4

5

6

7

8

Left lateral paratergites missing before burial

9

Grainy ornamentation to anterior edges of tergites

10

11

12 ?13

?14

POSTERIOR   20 cm

figure 3

figure 4

Approx. location of master fault

HT

C

B

A

Stainmore Formation

Howick master fault

Alston Formation

HT

D

figure 5

figure 6

figure 7

SLAB A

Smear A

Part A

Tergite and paratergite impressions

Syn-depositionally broken edge

Burrow

x

x'

Cordaitalean seeds same level as fossil

3-D cut shows thrusting of sand-filled tergites

Above: Sandstone
Top: mica/carbonaceous smear
Bottom: surface of Slab A
Below: Slab B

SLAB A

SLAB B

Contiguous cross-bed set fractured along fossil-bearing plane

Sediment doming in Slab B

Burrow

Syn-depositionally broken edge

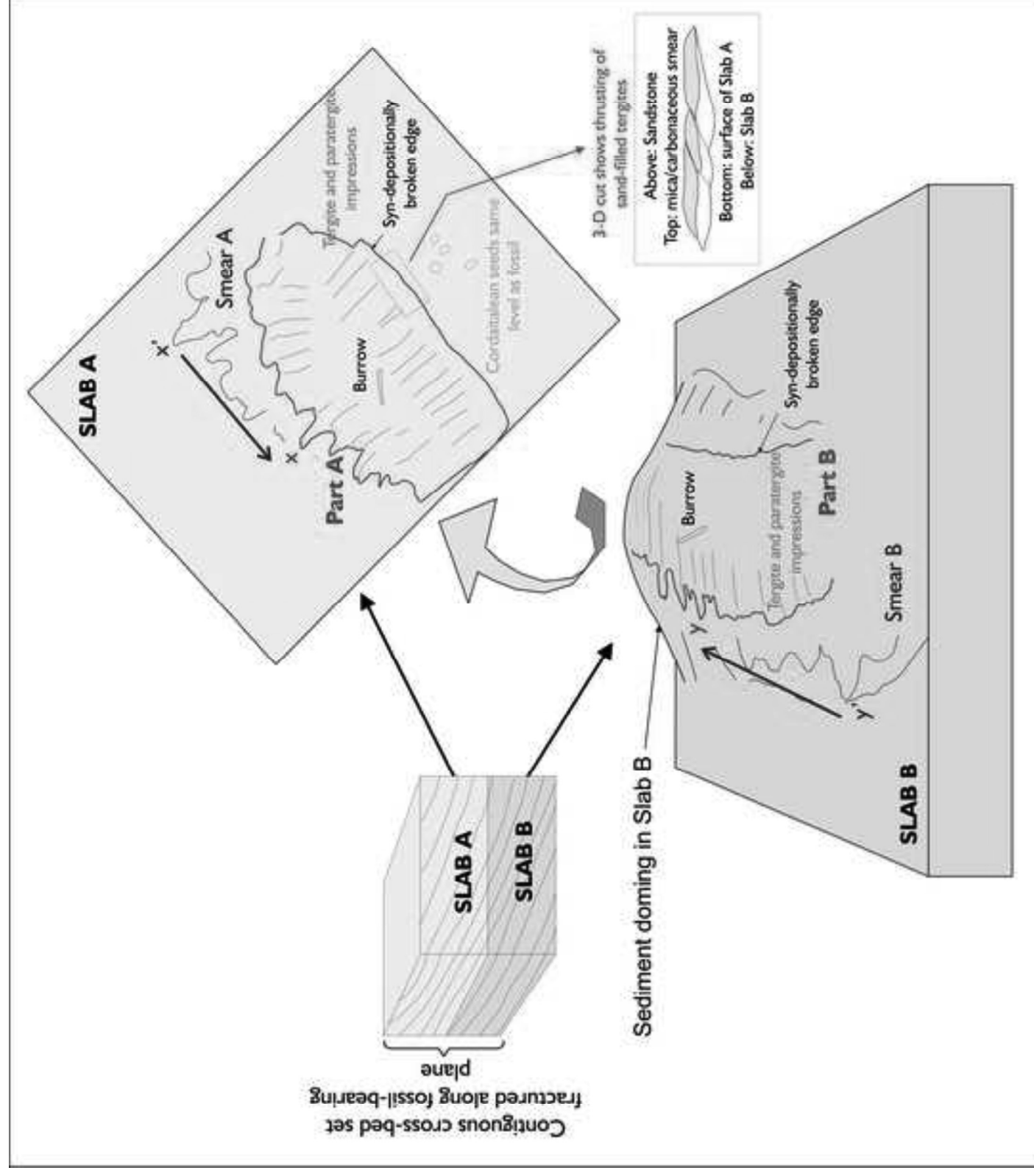Part B

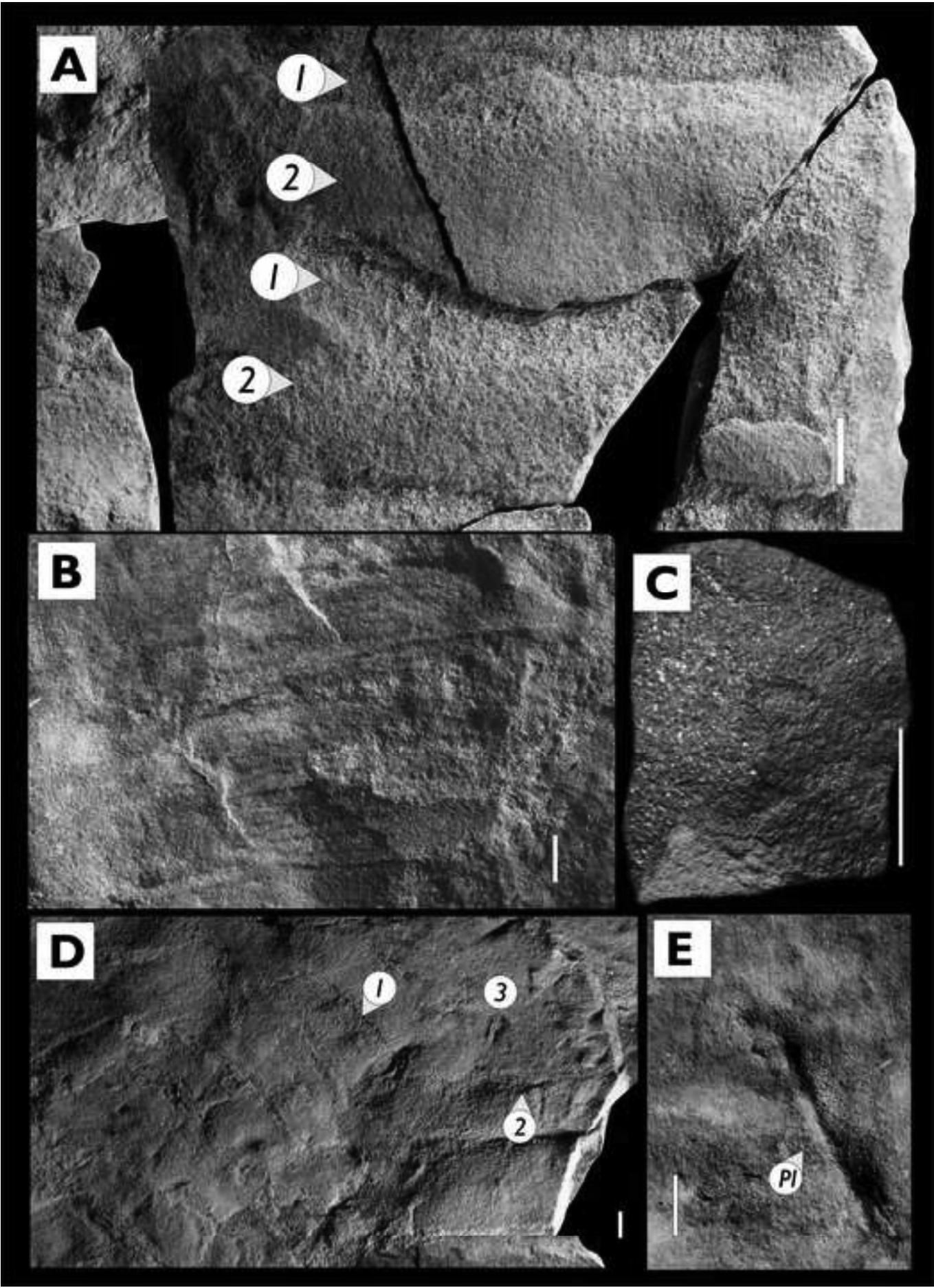Tergite and paratergite impressions

Smear B

y

y'

SLAB B

figure 8

figure 9
Click here to access/download;figure;Art resub F9.jpg ±

figure 10
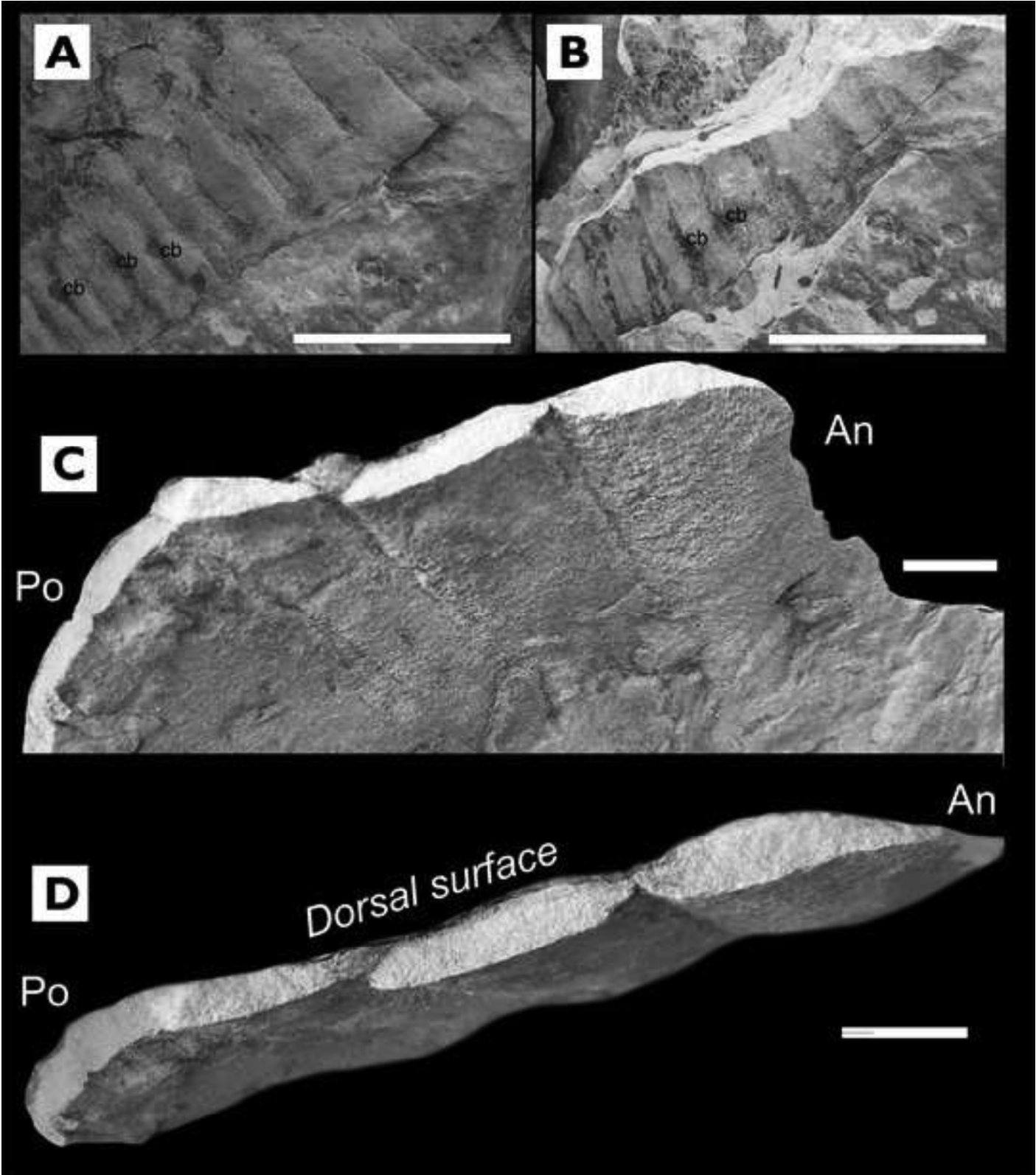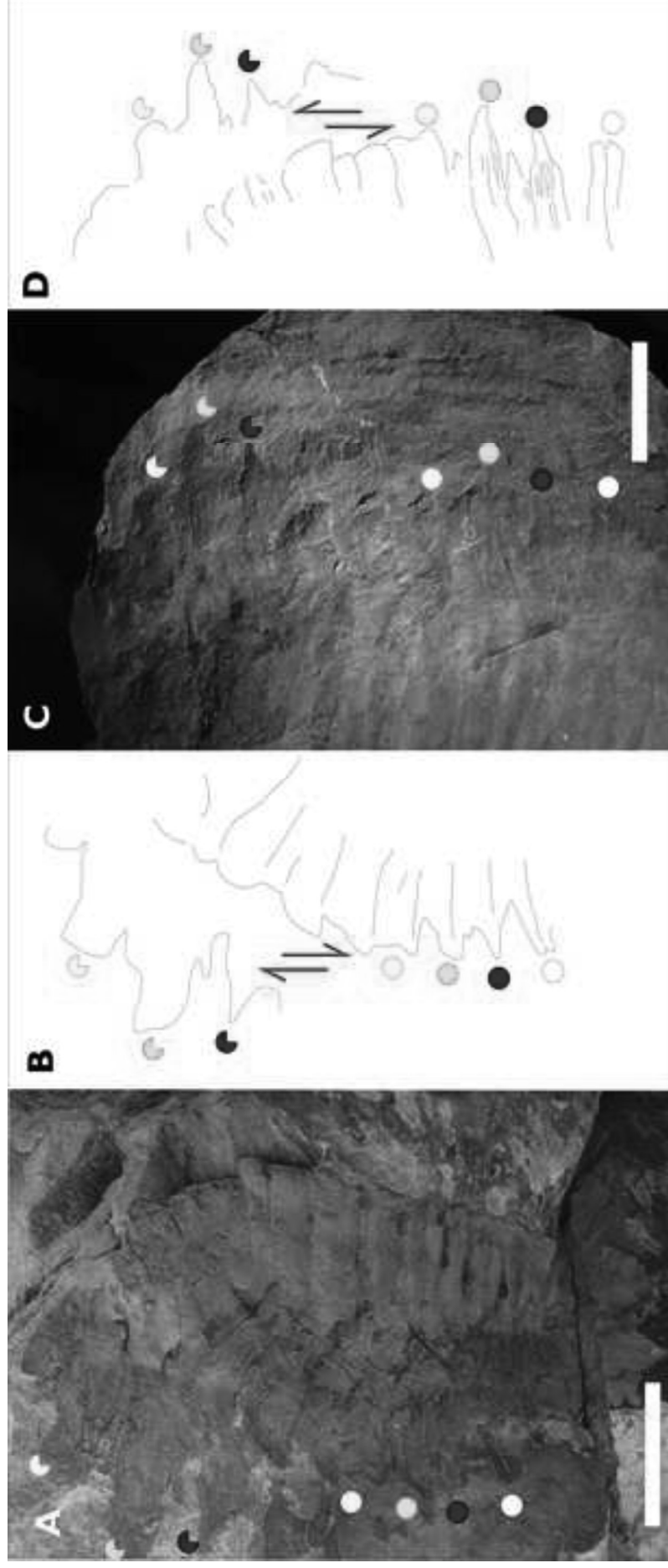
figure 11

A

Stainmore Formation (Serpukhovian)
Howick Bay, Northumberland, UK
Specimen size: L: 76 cm / W: 36 cm
12-14 tergites
Estimated animal length: 2.63 m

Sulzbach Formation (Moscovian)
Maybach mine, Saarland, Germany
Specimen size: L: 85 cm / W: 23 cm
26-27 tergites
Estimated animal length: 1.1 m

Döhlen Formation (Gzhelian-Asselian)
Döhlen Basin, Saxony, Germany
Specimen size: L: 42 cm / W: 18 cm
25 ventral segments
Estimated animal length: 0.65-0.8 m

50 cm

B

Visean:
Pittenweem Fm
Kingsbarns, Fife, UK
Width 50 cm
Est. animal length: 2.4 m

Serpukhovian:
Limestone Coal Fm
Arran, Bute, UK
Width 36 cm
Est. animal length: 1.7 m

Bashkirian:
Tynemouth Creek Fm
Gardner Creek, NB, Canada
Width 30 cm
Est. animal length: 1.4 m

Moscovian:
Malagash Fm
Pugwash, NS, Canada
Width 41 cm
Est. animal length: 1.9 m

Gzhelian:
Cape John Fm
Cape John, NS, Canada
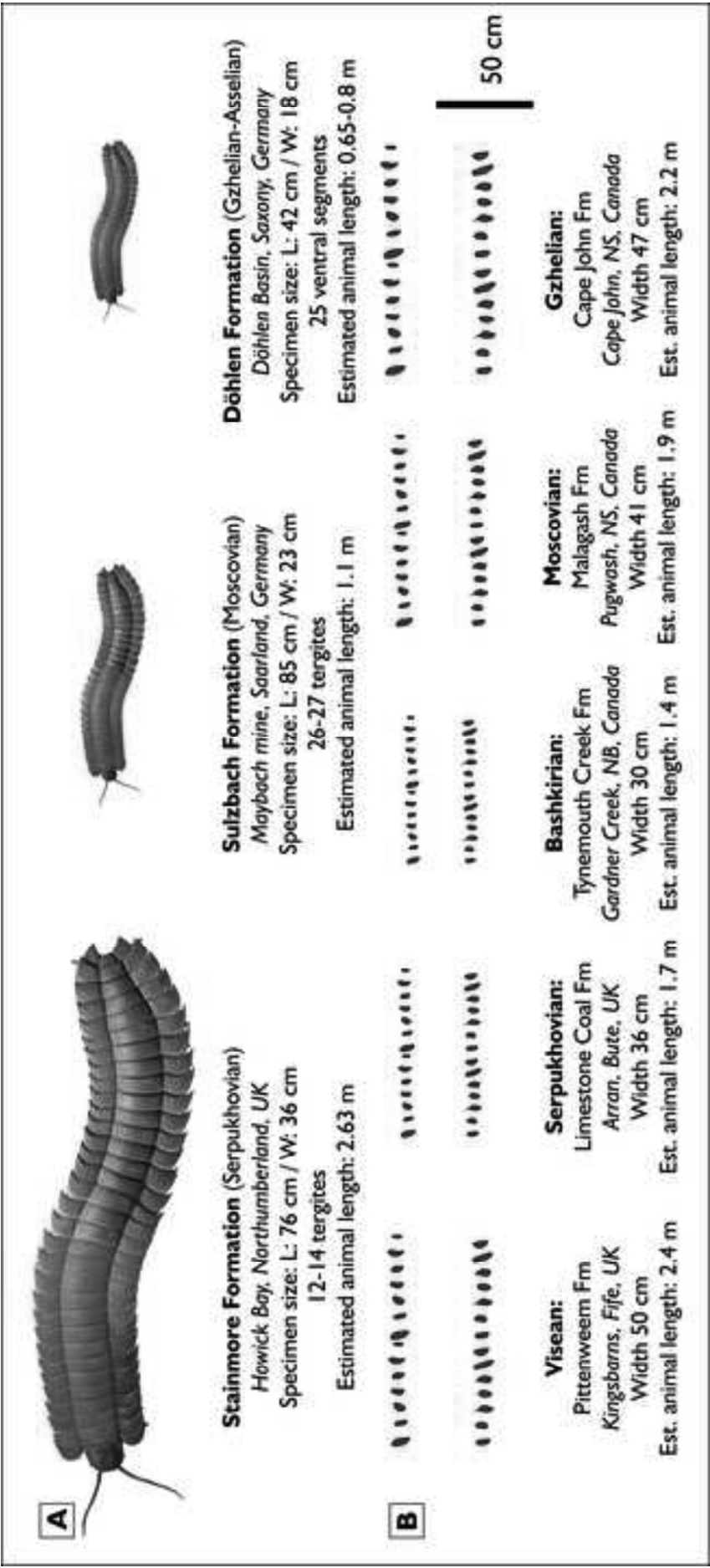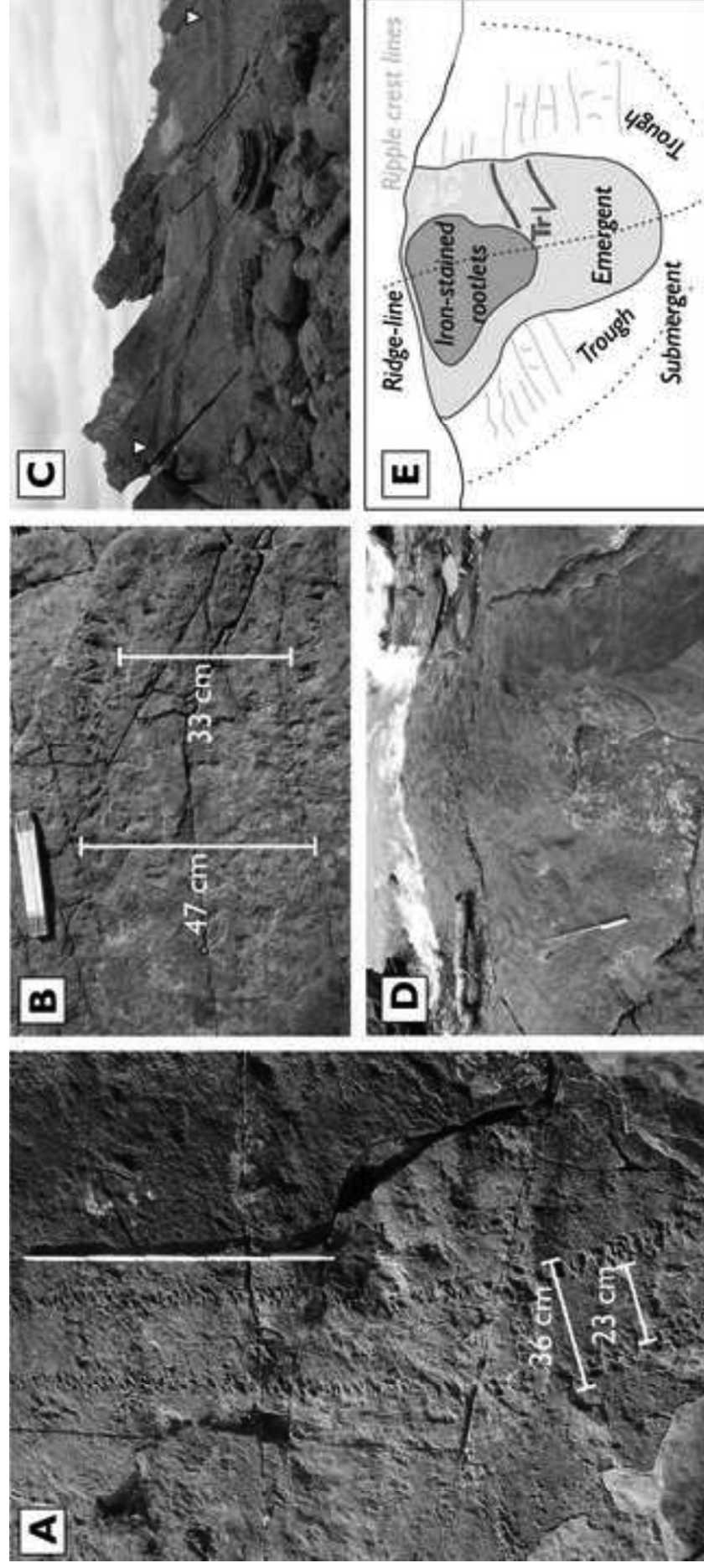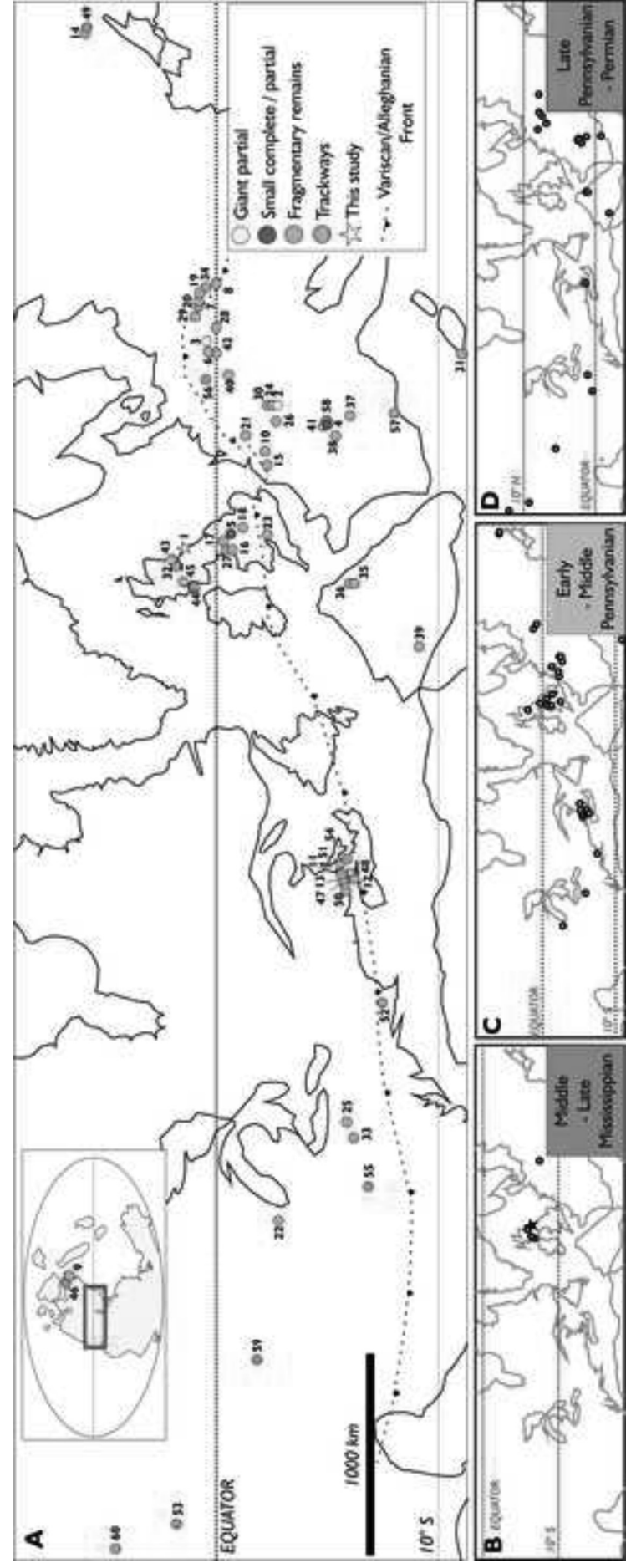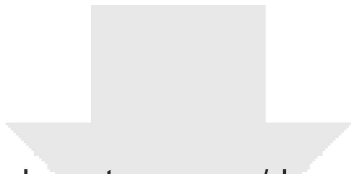Width 47 cm
Est. animal length: 2.2 m

figure 12

figure 13

Click here to access/download
supplementary material
Arthropleura SI 03-09-21.docx